JOURNAL OF GEOPHYSICAL RESEARCH: SPACE PHYSICS, VOL. 118, 1–21, doi:10.1002/jgra.50096, 2013

# Structure of Titan's induced magnetosphere under varying background magnetic field conditions: Survey of Cassini magnetometer data from flybys TA–T85

Sven Simon,[1] Shari C. van Treeck,[1] Alexandre Wennmacher,[1] Joachim Saur,[1] Fritz M. Neubauer,[1] Cesar L. Bertucci,[2] and Michele K. Dougherty[3]

Received 15 October 2012; revised 20 December 2012; accepted 21 December 2012.

[1] Cassini magnetic field observations between 2004 and 2012 suggest the ambient field conditions near Titan's orbit to differ significantly from the frequently applied pre-Cassini picture (background magnetic field homogeneous and perpendicular to Titan's orbital plane, stationary upstream conditions). In this study, we analyze the impact of these varying background field conditions on the structure of Titan's induced magnetosphere by conducting a systematic survey of Cassini magnetic field observations in the interaction region during flybys TA–T85 (July 2004–July 2012). We introduce a set of criteria that allow to identify deviations in the structure of Titan's induced magnetosphere—as seen by the Cassini magnetometer (MAG)—from the picture of steady-state field line draping. These disruptions are classified as "weak", "moderate", or "strong". After applying this classification scheme to all available Titan encounters, we survey the data for a possible correlation between the disruptions of the draping pattern and the ambient magnetospheric field conditions, as characterized by *Simon et al*. [2010a]. Our major findings are: (1) When Cassini is embedded in the northern or southern lobe of Saturn's magnetodisk within a $\pm 3$ h interval around closest approach, Titan's induced magnetosphere shows little or no deviations at all from the steady-state draping picture. (2) Even when Titan is embedded in perturbed current sheet fields during an encounter, the notion of draping the average background field around the moon's ionosphere is still applicable to explain MAG observations from numerous Titan flybys. (3) Only when Titan is exposed to intense north-south oscillations of Saturn's current sheet at the time of an encounter, the signatures of the moon's induced magnetosphere may be completely obscured by the ambient field perturbations. (4) So far, T70 is the only flyby that fully meets the idealized pre-Cassini picture of the Titan interaction (steady background field perpendicular to Titan's orbital plane, steady upstream flow, unperturbed induced magnetosphere).

**Citation:** Simon, S., S. C. van Treeck, A. Wennmacher, J. Saur, F. M. Neubauer, C. L. Bertucci, and M. K. Dougherty (2013), Structure of Titan's induced magnetosphere under varying background magnetic field conditions: Survey of Cassini magnetometer data from flybys TA–T85, *J. Geophys. Res. Space Physics*, *118*, doi:10.1002/jgra.50096.

## 1. Introduction

[2] Since the arrival of Cassini in the Saturnian system in 2004, observations from more than 80 close flybys have greatly enriched our understanding of the interaction between Saturn's largest moon Titan (radius $R_T = 2575$ km) and its magnetospheric plasma environment. Due to the absence of a significant intrinsic magnetic field [*Neubauer et al*., 1984; *Backes et al*., 2005; *Wei et al*., 2010], Titan's ionosphere is subject to direct erosion by the incident plasma flow. This interaction generates an induced magnetosphere around the moon: the ambient magnetospheric field drapes around Titan's ionosphere, leading to the formation of a magnetic pile-up region at the ramside and a bipolar magnetotail in the wake region. Ionospheric particles are swept out of the interaction region by the electromagnetic fields of the incident plasma, with their gyroradii exceeding the radius of Titan by up to an entire order of magnitude [*Luhmann*, 1996; *Simon et al*., 2007a].

[3] In the pre-Cassini era and also after the arrival of the spacecraft at Saturn, the Titan interaction has frequently been described in terms of the idealized picture deduced from a single flyby of Voyager 1 in 1980. In this description,

[1]Institute of Geophysics and Meteorology, University of Cologne, Germany.
[2]Institute for Astronomy and Space Physics, CONICET/University of Buenos Aires, Ciudad Universitaria; Buenos Aires, Argentina.
[3]Space and Atmospheric Physics Group, The Blackett Laboratory, Imperial College London, UK.

Corresponding author: Simon, Sven, Institute of Geophysics and Meteorology, University of Cologne; Germany. (simon@geo.uni-koeln.de)


2169-9380/13/10.1002/jgra.50096

the ambient magnetospheric field $\underline{B}_0$ was assumed to be perpendicular to Titan's orbital plane. Besides, the incident plasma and magnetic field conditions were considered to remain constant on the length and time scales upon which the interaction process takes place. These scales are defined by, e.g., the transit time of the incident plasma through the interaction region or by the gyroradii/gyroperiods of the involved ion species. In addition, most available models of the Titan interaction assume the incident flow velocity $\underline{u}_0$ to be aligned with the direction of ideal corotation, see, e.g., *Kallio et al*. [2004], *Backes et al*. [2005], and *Simon et al*. [2006]. In recent years, however, plasma and magnetic field data collected during Cassini's close encounters of Titan have revealed that this idealized set of upstream conditions may not reflect the real situation at all.

[4] On the one hand, the presence of Saturn's magnetodisk current sheet and the large-scale seasonal variations in its shape frequently place Titan's orbit in an environment where the radial (Saturn–Titan) component of the ambient magnetospheric field clearly dominates its north-south component [*Arridge et al*., 2008a, 2008b; *Bertucci et al*., 2009; *Simon et al*., 2010a, 2010b]. In Saturnian southern summer when the Cassini prime mission took place, Titan was on average located below the giant planet's magnetic equator, i.e., the moon was embedded in the southern lobe of the magnetodisk where the field points towards Saturn [*Simon et al*., 2010a, 2010b]. After equinox on 09 August 2011, the situation was reversed, and Titan's orbit could on average be found north of Saturn's magnetic equator. Furthermore, the deviation of the magnetospheric plasma velocity $|\underline{u}_0|$ in Titan's orbital plane from full corotation speed leads to a sweepback of the field lines with respect to a strictly corotating meridional plane, i.e., the flow-aligned component of the background field does not vanish either [*Bertucci et al*., 2009; *Wei et al*., 2009; *Simon et al*., 2010a].

[5] On the other hand, the magnetodisk near Titan's orbit is not a stationary structure, but it was found to carry out intense north-south oscillations around an average position, leading to perturbations of the ambient magnetospheric field near Titan on timescales between only a few minutes and up to 5 h (i.e., about half the planetary rotation period), see *Arridge et al*. [2008b, 2011a] for details. *Simon et al*. [2010a] showed that at least during the first five years of the Cassini mission (October 2004–October 2009, Titan flybys TA–T62), there was not a single Titan flyby during which the ambient magnetic field conditions matched the idealized picture deduced in the pre-Cassini era.

[6] The high variability of the ambient magnetospheric flow conditions causes significant deviations of the field signatures seen in Titan's interaction region by the Cassini magnetometer (MAG, *Dougherty et al*. [2004]) from the idealized picture of steady-state field line draping around the moon's ionosphere. Especially, *Neubauer et al*. [2006] found that below an altitude of about 1800 km, the plasma flow speed drops to values of only 100 m/s (compared to about 100 km/s in the incident plasma), while the magnetic Reynolds number still remains sufficiently high to insure validity of the frozen-flux theorem. Thus, a magnetic fluxtube which has been convected into this region can remain trapped there for up to several hours. These trapped fluxtubes were referred to as "fossil" magnetic fields by *Neubauer et al*. [2006]. A release of the trapped magnetic fluxtubes may occur at altitudes below about 1000 km, where magnetic diffusion becomes the predominant process [*Cravens et al*., 2010]. The residence time of magnetic field lines in the vicinity of Titan is probably prolonged by their passage through the diffusion-dominated region [*Neubauer et al*., 2010]. First observational evidence for the presence of fossil magnetic fields at Titan was found by *Bertucci et al*. [2008] who showed that during the T32 flyby, Titan had carried such a bundle of trapped fluxtubes from Saturn's magnetosphere into the magnetosheath.

[7] Hence, even if a stationary background field is observed during a certain Titan flyby, a "contamination" of the interaction region by fossil field signatures may still be present, recording the moon's exposure to previously encountered, different field regimes. Such signatures will cause disruptions of the draping signature at low altitudes which cannot be explained in terms of Titan's interaction with the momentary background field. *Cravens et al*. [2010] also suggested that below altitudes of about 1300 km, neutral winds may make a non-negligible contribution to the transport of the ionospheric magnetic field, thereby generating additional deviations from the idealized picture of steady-state field line draping.

[8] In recent years, several efforts have been made to systematically categorize the variability of the ambient magnetospheric plasma and field conditions near Titan's orbit. Based on data from the Cassini electron spectrometers, *Rymer et al*. [2009] presented a classification of Titan's plasma environment during flybys TA–T55. These authors grouped the electron background observed around the Titan encounters in four categories: plasma sheet, magnetodisk lobe, magnetosheath, and bimodal (i.e., a mixture of two easily identifiable, distinct electron populations). The results presented by *Rymer et al*. [2009] indicate the electron background near Titan's orbit to possess a high level of variability: only 34 encounters from the TA–T55 series could be clearly associated with one of these categories, whereas the remaining ones needed to be characterized by a combination of different environments. The findings of *Rymer et al*. [2009] were recently confirmed by a survey of ion data from the Cassini Plasmaspectrometer [*Németh et al*., 2011].

[9] In a companion study, *Simon et al*. [2010a] focused on the ambient magnetic field conditions during Titan flybys TA–T62 by applying a classification scheme that allows an unbiased discrimination between current sheet and lobe-type fields. These authors identified only ten encounters during which the background field within a $\pm 3$ h interval around closest approach (C/A) to Titan was not perturbed by Saturn's highly dynamic current sheet. It was also demonstrated that Titan itself does not exert a measurable level of control on the motion of Saturn's current sheet near its orbit [*Simon et al*., 2010b]. A comparative discussion of the available classification studies was recently provided by *Arridge et al*. [2011b].

[10] While significant efforts have been made to characterize the variability of the ambient plasma and magnetic field conditions near Titan's orbit, the influence of the time-varying magnetospheric environment on the structure of the moon's induced magnetosphere is so far only poorly constrained. Several real-time simulation studies focused on the transitions in Titan's plasma environment when the moon moves from

one steady-state magnetic field regime to another, e.g., during a passage through Saturn's magnetopause as observed during the T32 flyby [*Simon et al*., 2009a; *Ma et al*., 2009; *Müller et al*., 2010]. These authors found the lifetime of fossil fields in Titan's ionosphere to reach values of at least $2-3$ h. *Simon et al*., [2008a] presented a first hybrid (kinetic ions, fluid electrons) simulation study that placed Titan within an oscillatory background magnetic field, fluctuating on a time scale comparable to the ion gyroperiods. They demonstrated that the slow and dense heavy ion plasma around Titan can—to a certain degree—shield the induced magnetosphere against changes in the ambient magnetic field orientation.

[11] The purpose of the present study is to make a further step towards understanding the impact of time-varying background magnetic field conditions on the structure of Titan's induced magnetosphere. However, while the preceding studies [*Simon et al*., 2008a, 2009b; *Ma et al*., 2009; *Müller et al*., 2010] applied simplified numerical models to gain basic insights into the involved physical processes, our approach in the present work is based on an observational point of view. By conducting a survey of Cassini magnetic field observations from all Titan flybys between Saturn Orbit Insertion in July 2004 and the time of this writing (fall 2012, flybys TA–T85), we intend to identify all encounters during which the structure of Titan's induced magnetosphere revealed significant deviations from the idealized picture of steady-state draping of the average background field. In order to allow an unbiased characterization of the magnetic field signatures seen *within Titan's induced magnetosphere*, we introduce a set of classification criteria, in analogy to what *Simon et al*. [2010a, 2010b] did for the *ambient field conditions near Titan's orbit*. Subsequently, we shall look for a possible correlation between the disruptions observed within Titan's induced magnetosphere and the well characterized ambient magnetospheric field conditions.

[12] This study is organized as follows: in section 2, we briefly update the classification table for the ambient magnetospheric field conditions by including Titan flybys T63–T85, which were accomplished by Cassini after publication of eSimonflybys. Thus, the required classification information on the background field will be available for the entire TA–T85 series. Section 3 then introduces a set of criteria that allow to characterize the deviations of the field signatures observed within Titan's induced magnetosphere from the steady-state draping picture. By applying this classification scheme to a series of selected Titan flybys, its validity is demonstrated in section 4. Subsequently, we provide the classification results for Titan's induced magnetosphere during all available Cassini encounters (cf. section 5) and discuss the implications of our results and a possible correlation to the ambient magnetospheric field conditions (cf. section 6). The study concludes with a brief summary of our major findings in section 7.

[13] Within the framework of this study, two coordinate systems are applied to display the magnetic field data: the *Titan Interaction System* (TIIS) which is denoted by small letters ($x$,$y$,$z$) and the *Draping Coordinate System* (DRAP), the axes of which are labeled with capital letters ($X$,$Y$,$Z$). The origins of both coordinate frames coincide with the center of Titan. The ($+x$) axis of the TIIS is aligned with the direction of ideal corotation, whereas the ($+y$) axis points from Titan to Saturn. The ($+z$) axis completes the right-handed coordinate system, pointing northward (i.e., it is approximately parallel to Saturn's magnetic moment/rotation axis). The DRAP system will be introduced in section 3.1. The unit vectors of the two coordinate frames are referred to as $\{\underline{e}_x, \underline{e}_y, \underline{e}_z\}$ for TIIS and $\{\underline{e}_X, \underline{e}_Y, \underline{e}_Z\}$ for DRAP, respectively.

## 2. Titan's Magnetospheric Environment During Flybys T63–T85

[14] In our two preceding studies [*Simon et al*., 2010a, 2010b], we have classified the ambient magnetic field conditions during Titan flybys TA–T62 as well as during their "virtual" counterparts (i.e., during crossings of Titan's orbit that occurred when the moon and the spacecraft were located in different local time sectors of the magnetosphere). To complete our picture of Titan's magnetospheric environment, we now apply the same classification technique to the magnetospheric background fields during the subsequent Titan flybys T63–T85. In the course of this analysis, we finally obtain a complete local time coverage of the ambient field conditions near Titan's orbit: while at the time of our initial study, T34 was the only encounter available in the dusk magnetosphere (15:00–21:00 Saturnian local time), this gap is now filled by Titan encounters T63–T74, T76, T78, T80, and T82.

[15] The classification technique applied to the magnetospheric background field has been discussed in detail in our two preceding publications (cf. section 2 in *Simon et al*. [2010a] and section 2.2 in *Simon et al*. [2010b]). Therefore, we will provide only a very brief overview of the key elements here. We apply the ratio of the average radial component ($B_y$ in TIIS coordinates) to the average field strength $B \equiv |\underline{B}|$ as well as the standard deviation $\delta B_y$, calculated within intervals of 1 h length, for a discrimination between current sheet and lobe-type fields. A field regime that fulfills the two conditions

$$\frac{|B_y|}{B} > 0.6 \qquad \text{and} \qquad \frac{\delta B_y}{B} < 0.05 \tag{1}$$

is assigned to the northern magnetodisk lobe regime (symbol $L^N$), if $B_y$ is negative and to the southern magnetodisk lobe regime (symbol $L^S$), if $B_y$ is positive. The current sheet regime (symbol *Sh*) is identified either by a breakdown of the first criterion (i.e., $\frac{|B_y|}{B} < 0.6$), or by a normalized fluctuation level above $\frac{\delta B_y}{B} = 0.2$. Of course, a magnetic field regime that simultaneously fulfills $\frac{|B_y|}{B} < 0.6$ and $\frac{\delta B_y}{B} > 0.2$ is assigned to the current sheet as well. The transition regime

$$\frac{|B_y|}{B} > 0.6 \qquad \text{and} \qquad 0.05 < \frac{\delta B_y}{B} < 0.2 \tag{2}$$

is classified as a slightly perturbed lobe regime (symbols $L^N_{Sh}$ for the northern lobe and $L^S_{Sh}$ for the southern lobe).

[16] Our classification results for the ambient field conditions within a $\pm 8$ h interval around C/A of T63–T85 are provided in Table 1. Overall, these results confirm the picture of a perturbed magnetic environment near Titan, as deduced in our preceding study [*Simon et al*., 2010a] for the TA–T62 flyby series. There is not a single encounter in the T63–T85 series during which quiet, lobe-type fields were observed on both sides of C/A. During 17 encounters, Cassini was embedded in current sheet fields within a $\pm 3$ h interval around C/A, whereas only five flybys featured lobe-type fields

**Table 1.** Classification of Titan's Magnetic Environment During Cassini Flybys T63–T85[a]

| Flyby | Date | SLT | Class. inb. | Class. outb. |
|---|---|---|---|---|
| T63 | 12 Dec 2009 | 17.0 | *Sh* | *Sh*, $L^S_{Sh}$, *Sh* |
| T64 | 28 Dec 2009 | 17.0 | *Sh* | *Sh*, $L^S_{Sh}$, *Sh* |
| T65 | 12 Jan 2010 | 16.9 | $L^N_{Sh}$, *Sh*, $L^S_{Sh}$ | *Sh*, $L^N_{Sh}$, *Sh* |
| T66 | 28 Jan 2010 | 17.0 | *Sh* | *Sh* |
| T67 | 05 Apr 2010 | 21.1 | *Sh* | *Sh*, $L^S_{Sh}$, *Sh*, $L^S_{Sh}$, *Sh* |
| T68 | 20 May 2010 | 16.1 | *Sh*, $L^S_{Sh}$ | *Sh*, $L^N_{Sh}$, *Sh* |
| T69 | 05 Jun 2010 | 16.1 | *Sh*, $L^N_{Sh}$, *Sh* | *Sh*, $L^N_{Sh}$, *Sh*, $L^N_{Sh}$ |
| T70 | 21 Jun 2010 | 16.1 | *Sh* | *Sh* |
| T71 | 07 Jul 2010 | 16.1 | $L^N_{Sh}$, *Sh*, $L^N_{Sh}$, *Sh* | *Sh* |
| T72 | 24 Sep 2010 | 16.0 | *Sh* | *Sh*, $L^S_{Sh}$, *Sh* |
| T73 | 11 Nov 2010 | 15.8 | *Sh*, $L^N_{Sh}$, *Sh*, $L^N_{Sh}$, *Sh* | *Sh* |
| T74 | 18 Feb 2011 | 20.6 | *Sh*, $L^N_{Sh}$, $L^N$, $L^N_{Sh}$, *Sh* | *Sh*, $L^N_{Sh}$, $L^N$, $L^N_{Sh}$ |
| T75 | 19 Apr 2011 | 14.2 | *Sh* | *Sh* |
| T76 | 08 May 2011 | 19.8 | *Sh* | *Sh*, $L^N_{Sh}$, *Sh*, $L^N_{Sh}$, *Sh* |
| T77 | 20 Jun 2011 | 12.2 | *Sh* | *Sh* |
| T78 | 12 Sep 2011 | 17.5 | *Sh* | *Sh* |
| T79 | 13 Dec 2011 | 12.9 | *Sh*, $L^N_{Sh}$, *Sh*, $L^N_{Sh}$ | *Sh* |
| T80 | 02 Jan 2012 | 18.6 | $L^N_{Sh}$, *Sh* | *Sh*, $L^N_{Sh}$, *Sh*, $L^S_{Sh}$ |
| T81 | 30 Jan 2012 | 12.6 | *Sh*, $L^N_{Sh}$ | *Sh*, $L^N_{Sh}$, *Sh* |
| T82 | 19 Feb 2012 | 18.4 | *Sh*, $L^N_{Sh}$, *Sh* | *Sh*, $L^N_{Sh}$ |
| T83 | 22 May 2012 | 13.7 | $L^N_{Sh}$, *Sh* | $L^N_{Sh}$, *Sh* |
| T84 | 07 Jun 2012 | 13.7 | $L^N_{Sh}$, *Sh* | *Sh* |
| T85 | 24 Jul 2012 | 13.6 | *Sh*, *Msh*, *Sh*, *Msh* | *Msh*, *SW*, *Msh* |

[a]The classification scheme discriminates between the inbound (inb.) and the outbound (outb.) region of each flyby. For each encounter, an interval of about ±8 h around Closest Approach (C/A) is considered. A transition between different magnetic field regimes (as observed, e.g., during T65) is denoted by a sequence of classification symbols in chronological order. For each flyby, the last symbol in the "Inbound" column and the first symbol in the "Outbound" column characterize the magnetic field conditions that prevailed within a window of roughly ± 3 h around C/A. The table also provides the Saturnian Local Time (SLT) at the position of Titan during each encounter. T85 is the third Titan flyby of the Cassini mission during which Titan was found within Saturn's magnetosheath ("*Msh*"). About 3 h after C/A, Cassini entered the unperturbed Solar Wind ("*SW*") upstream of saturn's bow shock.

on one side of C/A. In analogy to the preceding Titan flybys T52–T62 [*Simon et al*., 2010a, section 5.2], magnetic field data from several encounters reveal rapid changes between lobe-type and current sheet fields, pointing towards an intense north-south oscillatory motion of the sheet around Titan's orbital plane. The seasonal changes in the global structure of Saturn's magnetosphere during the three years covered by T63–T85 also manifest in the Titan flyby data: the more time has passed since equinox on 11 August 2009, the fewer detections of southern lobe-type fields occur within the ± 8 h interval. In northern spring/summer (after equinox), the shape of Saturn's magnetodisk current sheet can be described by an upended bowl [*Arridge et al*., 2008b], i.e., the boundary between northern and southern lobe-type fields is on average displaced to south of Titan's orbital plane.

[17] A very special encounter in the T63–T85 series is T70. On the one hand, the spacecraft achieved the smallest C/A altitude (878.1 km) of all Titan flybys scheduled during Cassini's tour in the Saturnian system. On the other hand, there is so far no other Titan flyby for which the current sheet regime was identified by the $\frac{|B_y|}{B} < 0.6$ criterion alone: while the $B_y$ component remained negligibly small within the entire ± 8 h interval—i.e., the background field was oriented mainly in ($-z$) direction—the normalized fluctuation level remained below $\frac{\delta B_y}{B} < 0.2$ during that period. Thus, among all available Titan encounters of the Cassini mission, T70 is the so far only one which matches the idealized background magnetic field conditions frequently applied in the pre-Cassini era ($\underline{B}_0$ homogeneous, stationary, and perpendicular to Titan's orbital plane) reasonably well. The magnetic field observations acquired during T70 are displayed in Figure 3 and will be subject of a detailed discussion in section 4.1.

## 3. Titan's Induced Magnetosphere: Classification Technique

[18] To gain straightforward access to the observed interaction features, MAG data from the Titan flybys are transformed to the DRAP system introduced in section 3.1. The method applied to analyze the datasets is then described in section 3.2.

### 3.1. Draping Coordinate System (DRAP)

[19] As discussed in the preceding sections, there are numerous Titan flybys during which the average background field was *not* antiparallel to the $z$ axis of the TIIS. When Titan is located in the northern lobe of Saturn's magnetodisk, the incident magnetic field $\underline{B}_0 = \left(B_{0,x}, B_{0,y}, B_{0,z}\right)$ possesses a negative $B_{0,y}$ component (i.e., it is directed away from Saturn) as well as a negative $B_{0,x}$ component (i.e., the field lines are swept back with respect to a strictly corotating meridional plane). In the southern magnetodisk lobe, the signs of both, $B_{0,x}$ and $B_{0,y}$ are reversed [*Bertucci et al*., 2009; *Simon et al*., 2010a].

[20] As shown, e.g., by *Simon et al*. [2007b, 2008b], a finite $B_{0,y}$ component gives rise to a rotation of Titan's induced magnetosphere around the corotational flow direction $\underline{e}_x$. If $B_{0,y}$ is positive, the interaction signatures are rotated around the ($+x$) axis in clockwise direction, whereas in the case of negative $B_{0,y}$, a counter-clockwise rotation occurs.

[21] Besides, a finite flow-aligned field component in the incident magnetospheric plasma generates an asymmetry of the induced magnetosphere with respect to the ($z = 0$) plane, in addition to the asymmetries between Saturn-facing and Saturn-averted hemisphere caused by large ion gyroradii. In the case of $B_{0,x} > 0$, Titan's magnetic lobes and the polarity reversal layer in between are shifted into the northern ($z > 0$) half space, while a negative $B_{0,x}$ yields a shift into the southern ($z < 0$) half space. The asymmetries arising from a finite $B_{0,x}$ component have been studied in detail by *Simon and Motschmann* [2009], who applied a hybrid simulation code to Titan's magnetospheric interaction.

[22] Hence, the TIIS is not suitable for illustrating the structure of Titan's induced magnetosphere when the background field is not aligned with the $z$ axis. Instead, we adopt the concept of a DRAP system ($X$,$Y$,$Z$), as introduced by *Neubauer et al*. [2006]. In the DRAP system applied in our study, the ($+Z$) axis is defined by the vector $(0, -B_{0,y}, -B_{0,z})$, thereby eliminating the influence of a rotation of the induced magnetosphere around the corotation direction. Thus, if the $B_{0,x}$ component of the ambient magnetic field vanishes, the ($Z = 0$) plane coincides with the location of the polarity reversal layer between Titan's northern (negative $B_x$ perturbation) and southern (positive $B_x$ perturbation) magnetic lobe. Of course, this statement is only valid under the assumption of $\underline{u}_0$ being aligned with the direction of corotation.

[23] At the time of this writing, reliable information on the incident magnetospheric flow direction near Titan during the Cassini flybys was not available in the peer-reviewed literature. Only for the T9 encounter—a passage through Titan's midrange magnetotail in 2005—an attempt had been made to derive the orientation of the incident flow vector from both plasma observations [*Szego et al.*, 2007 and magnetic field data [*Bertucci et al.*, 2007]. However, these two studies obtained vastly different results: while *Bertucci et al.* [2007] suggest that the ambient flow vector $\underline{u}_0$ during T9 was tilted *towards Saturn* at a constant angle of about 36°, *Szego et al.* [2007] identified significant changes in the direction of the incident plasma during the encounter. In some regions, they found $\underline{u}_0$ pointing *radially away from Saturn* at an angle of about 60°. Hence, a catalog of the ambient flow directions during the available Titan flybys is not only missing, but the analysis of T9 also suggests that it may be difficult to obtain a unique solution for $\underline{u}_0$ during a certain flyby from the available datasets. In the present study, we therefore apply a DRAP system whose (+*X*) axis is aligned with the direction of ideal corotation (i.e., $\underline{e}_X = \underline{e}_x$).

[24] Although *Arridge et al.* [2011c] could not provide velocity data for all the Titan flybys, they recently demonstrated that non-negligible radial and axial flow components may occur near Titan's orbit. In such a case, Titan's induced magnetosphere will no longer be "centered" around the corotation direction, but the general appearance of the draping pattern will remain unaffected.

[25] As will be discussed in sections 4 and 6, MAG data—displayed in DRAP coordinates—can be employed to identify those Titan flybys for which the assumption of a stationary upstream flow along the corotation direction may not be applicable.

[26] The (+*Y*) axis of the DRAP system completes the right-handed coordinate frame, i.e., $\underline{e}_Y = \underline{e}_Z \times \underline{e}_X$. In the case of $B_{0,X} \neq 0$, the polarity reversal layer between Titan's magnetic lobes is tilted with respect to the ($Z = 0$) plane, while it is still perpendicular to the ($Y = 0$) plane [*Simon and Motschmann*, 2009].

[27] In summary, the transformation of a magnetic field vector $\underline{B} = (B_x, B_y, B_z)$ from the TIIS (small letters) to the DRAP system (capital letters) reads as follows:

$$B_X = B_x \quad ; \tag{3}$$

$$B_Y = \frac{1}{\sqrt{B_{0,y}^2 + B_{0,z}^2}} \left(B_{0,y} B_z - B_{0,z} B_y\right) \quad ; \tag{4}$$

$$B_Z = -\frac{1}{\sqrt{B_{0,y}^2 + B_{0,z}^2}} \left(B_{0,y} B_y + B_{0,z} B_z\right) \quad , \tag{5}$$

where $\underline{B}_0 = (B_{0,x}, B_{0,y}, B_{0,z})$ denotes the background magnetospheric field in TIIS coordinates. The construction of the DRAP system from the TIIS is also illustrated in Figure 1.

[28] Hence, to transform the magnetic field signatures measured by Cassini from TIIS to DRAP, a background magnetospheric field $\underline{B}_0$ needs to be defined for each Titan encounter. To compute $\underline{B}_0$, we discriminate between the four categories of background magnetic field conditions introduced by *Simon et al.* [2010a]:

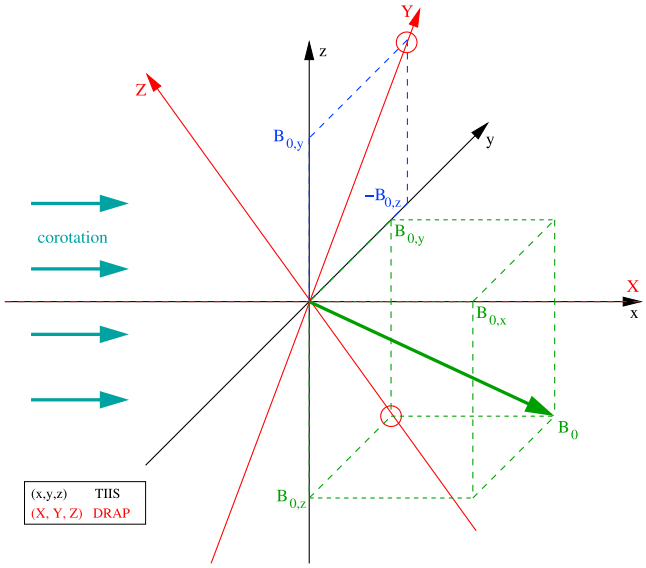


**Figure 1.** TIIS ($x, y, z$) and DRAP ($X, Y, Z$). In general, the background magnetospheric field $\underline{B}_0 = (B_{0,x}, B_{0,y}, B_{0,z})$ near Titan's orbit possesses three nonvanishing components. The (+*Z*) axis of the DRAP system is defined by the vector $(0, -B_{0,y}, -B_{0,z})$, i.e., it is located in the ($x = 0$) plane of the TIIS. The (+*X*) axis of the DRAP system coincides with the (+*x*) axis of the TIIS, defining the corotational flow direction. The (+*Y*) axis completes the right-handed, orthonormal DRAP system (i.e., $\underline{e}_Y = \underline{e}_Z \times \underline{e}_X$). Hence, the (+*Y*) axis points in the Saturn-facing half space, but it is inclined with respect to Titan's orbital plane ($z = 0$). The $B_{0,x}$ component of the ambient magnetospheric field is not considered for the definition of the DRAP system, since such an approach would not allow to define an orthogonal coordinate frame with one axis parallel to the corotation direction. In the scenario illustrated here, Titan was embedded in the southern lobe of Saturn's magnetodisk ($B_{0,y} > 0$), with the background field swept back with respect to full corotation ($B_{0,x} > 0$).

#### 3.1.1. Lobe-Type Fields on Both Sides of C/A (Abbreviation "*L–L*")

[29] During very few Titan flybys, Cassini detected quiet lobe-type fields of the same polarity in both, the inbound and the outbound region. For these encounters, we obtain $\underline{B}_0$ by calculating the average of the inbound and the outbound background field, as documented in Table 6 of *Simon et al.* [2010a] for TA–T62. As can be seen from Table 1 in the present study, the case of lobe-type fields on both sides of C/A did not reoccur during the later T63–T85 flybys.

#### 3.1.2. Lobe-Type Fields on One Side of C/A ("*L–Sh*" or "*Sh–L*")

[30] As can be seen from Table 5 in *Simon et al.* [2010a] and Table 1 of the present work, there are numerous Titan flybys during which quiet lobe-type fields were observed only on one side of C/A. On the other side, the MAG detected either perturbed current sheet fields [*Simon et al.*, 2010a, Figure 6], or an unambiguous discrimination between background field and features arising from Titan's local plasma interaction was not possible. The latter category is denoted by the asterisk symbol in the classification tables of our preceding paper. For these flybys, $\underline{B}_0$ has been

computed from a 2 h interval of the data collected on that side of C/A where quiet lobe-type fields were detected. Thus, the question that shall be addressed for this flyby category can be formulated as follows: if quiet lobe-type fields were detected only inbound *or* outbound of Titan, can this field still be applied to organize MAG observations within the moon's induced magnetosphere?

#### 3.1.3. Perturbed Current Sheet Fields on Both Sides of C/A ("*Sh–Sh*")

[31] For these flybys [T33, *Simon et al*., 2010a, Figure 10], the definition of a background field is problematic, since the ambient field conditions fluctuate on time scales of only a few minutes. However, one can nonetheless investigate whether the Titan interaction can still be adequately described by a steady-state draping of the *average* magnetic field around the obstacle. For this reason, we have computed an average background field $\underline{B}_0$ from two intervals of 120 min length inbound and outbound of the region perturbed by Titan's local magnetospheric interaction.

#### 3.1.4. Oscillatory Current Sheet

[32] Especially around equinox in August 2009, Cassini's C/A to Titan frequently coincided with intense north-south sweeps of Saturn's current sheet through the moon's orbital plane. After the magnetic field near Titan's orbit had remained nearly constant for several hours, the current sheet abruptly swept over the moon, going along with a polarity reversal in both $B_{0,x}$ and $B_{0,y}$. These polarity reversals occurred on time scales of about 1–3 h [*Simon et al*., 2010a]. During C/A of T52–T62, Titan was embedded in such transition regions, yielding strong gradients of the ambient magnetic field near its orbit and different signs of $B_{0,x}$ and $B_{0,y}$ on both sides of the interaction region [*Simon et al*., 2010a, section 5.2]. Similar characteristics of the ambient magnetospheric field were observed during several flybys of the T63–T85 series, cf. Table 1. For flybys of this category, the notion of Titan interacting with a constant background field is not applicable, i.e., the definition of a static DRAP system makes no sense. For our classification of the signatures detected within Titan's induced magnetosphere, a special set of classification criteria has therefore been applied to this type of encounter (see section 3.2).

### 3.2. Classification Criteria

[33] In this section, we introduce a classification scheme that allows to assess the deviations in the structure of Titan's induced magnetosphere (as observed by Cassini MAG) from the steady-state draping picture. Specifically, we shall consider (1) the agreement between expected and observed signs of the $B_x$ perturbations and (2) the magnitude of any superimposed disruptions compared to the primary draping signal. Each Titan flyby is assigned to one of four categories: "+," "(+)," "0," and "-." The deviations from the draping picture are small for "+," moderate for "(+)" and strong for "0." For a flyby characterized by the "-" symbol, the Titan interaction signature is not discernable in the magnetic field data, i.e., it is completely obscured by superimposed magnetospheric perturbations.

[34] For flybys that do *not* belong to the "oscillatory sheet" category, the classification scheme for Titan's induced magnetosphere works as follows: first, we transform the magnetic field data to the DRAP system. We then search an interval of $\pm 2$ h around C/A for signatures of the moon's induced magnetosphere. If no such signatures can be found, i.e., if the perturbations caused by Titan's local plasma interaction are either completely obscured by distortions in the ambient magnetospheric field or if there are no Titan-related perturbations at all imposed on a quiet magnetospheric background, the flyby is assigned to the "-" category.

[35] There are a few Titan flybys which occurred far upstream of the moon at a C/A altitude of about 1.4 $R_T$ or even larger (T66, T67, T72, T74, T79, T80). Since numerical simulations suggest the interaction signatures at these distances to be so weak that one would not expect them to exceed the background fluctuation level (e.g., *Ma et al*. [2006]; *Simon et al*. [2006, 2007a], see especially Figure 3b in the latter work), these flybys have been omitted in our analysis. For the same reason, the T81 flyby which occurred at an altitude of more than 12 $R_T$ downstream of the moon was not considered (cf. Figure 1d in *Ma et al*. [2011]). Thus, for the purposes of this study, the "Titan interaction region" is assumed to be located within a distance (along the $X$ axis) to the moon where the available models suggest the observable field disruptions to clearly exceed the noise level of about 0.1 $B_0$ that is always present in the background field.

[36] When the MAG instrument detected perturbations related to Titan's plasma interaction, there are two possibilities: first, if the sign of the observed $B_X$ perturbations is negative *or* positive throughout the interaction region, Cassini intersected only one "magnetic hemisphere" of the moon (i.e., the spacecraft remained either above or below the magnetic polarity reversal layer during the encounter). Second, during a flyby with a non-negligible north-south velocity component of the spacecraft, both magnetic lobes can be penetrated. The case of Cassini being completely embedded in the polarity reversal layer—i.e., $B_X$ remains unperturbed while $B_Z$ is enhanced at Titan's ramside and reduced at the wakeside—has not yet occurred.

[37] We examine the observed $B_X$ perturbations according to two criteria. First, we check whether the signs of the $B_X$ perturbations can be explained in terms of draping, see Figure 2 for illustration and *Simon and Motschmann* [2009]. If Titan was embedded in current sheet fields during the flyby, the $B_{0,X}$ component of the background field is approximately zero. In such a scenario, one expects to encounter regions with $B_X < 0$ only in Titan's northern hemisphere ($Z > 0$), whereas distorted regions with $B_X > 0$ should be confined to the ($Z < 0$) half space. The polarity reversal layer between both magnetic hemispheres then coincides with the ($Z = 0$) plane, cf. Figure 2a. Note that in this case, the DRAP system is identical to the TIIS.

[38] The situation becomes more complex when Titan was embedded in magnetodisk lobe-type fields around C/A. Although the background magnetospheric field (in DRAP coordinates) is then devoid of a finite $B_{0,Y}$ component, it still possesses a flow-aligned field component $B_{0,X} \neq 0$. In this case, the polarity reversal layer between Titan's two "magnetic hemispheres" is tilted with respect to the ($Z = 0$) plane, cf. Figures 2b and 2c for illustration. Most importantly, however, the polarity reversal layer does no longer retain its "flat" shape: while it is strongly tilted with respect to the ($Z = 0$) plane in the immediate vicinity of Titan, it becomes more and more aligned with the corotational flow direction at larger distances to the moon. *Simon and Motschmann*

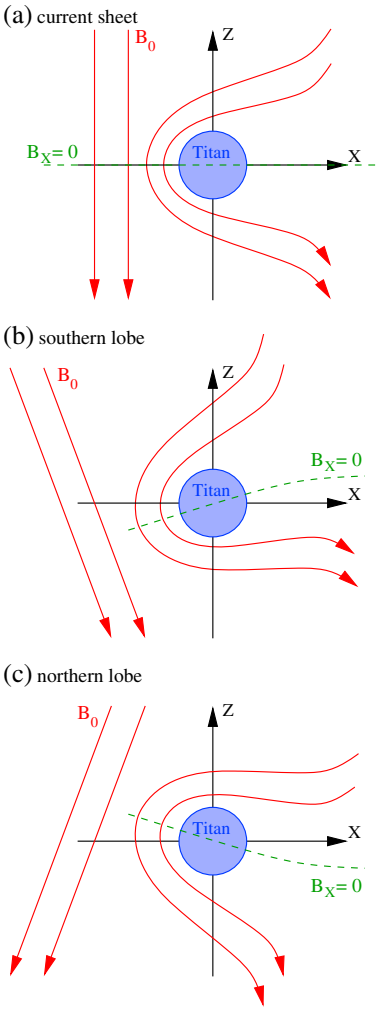


**Figure 2.** Titan's induced magnetosphere at different positions with respect to Saturn's current sheet. (a) When being embedded in Saturn's current sheet, both the $B_{0,X}$ and the $B_{0,Y}$ component at Titan's orbit (nearly) vanish, i.e., the background magnetospheric field is perpendicular to the direction of ideal corotation. In this case, the draping of the magnetic field (red lines) is symmetric with respect to the ($Z=0$) plane. Hence, the polarity reversal layer (green dashed line), separating regions of negative and positive $B_X$ perturbations, coincides with Titan's equatorial plane. (b) When Titan is located within the southern lobe of Saturn's magnetodisk, the ambient magnetospheric field possesses a positive $B_{0,X}$ component, yielding an asymmetrization of Titan's induced magnetosphere with respect to the ($Z=0$) plane. Downstream of Titan ($X>0$), the polarity reversal layer is now shifted in the northern ($Z>0$) half space, while in the upstream region ($X<0$), the polarity reversal of $B_X$ takes place in the ($Z<0$) half space. Besides, the polarity reversal layer now exhibits a curved shape: in the immediate vicinity of Titan, it is almost perpendicular to the background field, whereas it becomes more aligned with the corotation direction at larger distances to the moon. (c) When embedded in the northern lobe of Saturn's magnetodisk, the ambient magnetic field is tilted away from Titan (i.e., $B_{0,X}<0$). Thus, the polarity reversal layer downstream of Titan is now shifted to negative $Z$ values, while it can be found at positive values of $Z$ in the upstream region. The figure is a schematic illustration of the findings of *Simon and Motschmann* [2009].

[2009]) showed that the tilt of the polarity reversal layer against the ($Z=0$) plane remains always smaller than

$$\psi = arctan\left(\left|\frac{B_{0,X}}{B_{0,Z}}\right|\right) \tag{6}$$

(see Figures 1c, 4c, and 6c in their work), where $B_{0,X}$ and $B_{0,Z}$ denote the background field components in DRAP coordinates. Thus, the polarity reversal layer (for $B_{0,X}\neq 0$) is never strictly perpendicular to the magnetospheric background field.

[39] Let us focus on the case of Titan being located within the southern magnetodisk lobe during a flyby, as frequently encountered during the Cassini prime mission [*Bertucci et al.*, 2009; *Simon et al.*, 2010a]. In this scenario, the polarity reversal layer is shifted into the ($Z>0$) half space downstream of Titan and into the ($Z<0$) half space upstream of the moon, see Figure 2b. Hence, only the ($X<0, Z>0$) and the ($X>0, Z<0$) sectors can be assigned a well-defined polarity of the $B_X$ perturbations, whereas $B_X$ perturbations of both signs can be encountered in the ($X>0, Z>0$) and the ($X<0, Z<0$) sectors, containing the polarity reversal layer. We found that so far, all Titan flybys with a southern lobe-type $\underline{B}_0$ that crossed the ($X>0, Z>0$) or ($X<0, Z<0$) sectors and intersected only *one* of Titan's lobes well fulfilled the condition

$$|Z| \gg \left|\frac{B_{0,X}}{B_{0,Z}}\right| |X| \tag{7}$$

in these sectors. Therefore, one can formulate clear expectations on the sign of the $B_X$ perturbations for these flybys.

[40] If Cassini intersected both of Titan's lobes, we check whether the (bent) polarity reversal layer was crossed by the spacecraft in between the $Z=0$ plane and the $Z = \left|\frac{B_{0,X}}{B_{0,Z}}\right| X$ plane.

[41] As depicted in Figure 2c, a similar ambiguity may occur in Saturnian northern summer. However, a close flyby under northern magnetodisk lobe conditions that passed through the ($X>0, Z<0$) or the ($X<0, Z>0$) sector and did not cross Titan's polarity reversal layer has so far not been accomplished by Cassini. For the available flybys, we therefore checked whether Cassini crossed the polarity reversal layer between $Z=0$ and $Z = -\left|\frac{B_{0,X}}{B_{0,Z}}\right| X$.

[42] In summary, the first step of our classification scheme is to assess whether the signs of the observed $B_X$ perturbations agree ("↑," see also Table 2) or disagree ("↓") with the draping picture, as illustrated in Figure 2. We would like to emphasize again that the DRAP system is most suitable for a straightforward application of this analysis technique. In the TIIS, a nonvanishing $B_{0,y}$ component would rotate the induced magnetosphere around the $x$ axis. Thus, the polarity reversal layer is no longer perpendicular to the ($y=0$) plane, and the expressions that define "north" and "south" of the layer become far more complex. Even in the case of $B_{0,y}\neq 0$ and negligible $B_{0,x}$, the ($z=0$) plane would then no longer define the boundary between Titan's northern and southern magnetic hemispheres.

[43] We would like to note that another source of asymmetries—apart from a nonvanishing $B_{0,X}$ component—arises from the inclination of Titan's orbital plane with respect to the direction of the incident solar radiation. Between the TA encounter in October 2004 and T85 in July 2012, the latitude of Titan's subsolar point increased from $-23.2°$ to $+15.1°$.

**Table 2.** Classification Categories for Titan's Induced Magnetosphere[a]

| Sign($B_X$) | Add. Perturbations | Classification |
|---|---|---|
| ↑ | weak | + |
| ↑ | moderate | (+) |
| ↓ | weak | (+) |
| ↓ | moderate | 0 |
| ? | strong | 0 |

[a]The symbol in the first column indicates whether the signs of the observed $B_X$ perturbations agree ("↑") or disagree ("↓") with the draping picture (cf. Figure 2). The second column indicates whether additional perturbations that cannot be explained in terms of draping were superimposed on the interaction signature. In the case of "strong" additional perturbations, the deviations from the draping picture are so severe that the sign of the draped fields cannot be determined (denoted by the question mark). The third column contains the corresponding classification symbols.

However, as shown, e.g., by previous simulation studies of the T9 and the T34 encounters [*Simon et al*., 2007b, 2008b], a nonzero value of the solar zenith angle has negligible influence on the overall shape of the magnetic draping pattern, i.e., the location of the polarity reversal layer is mainly determined by the orientation of the ambient magnetospheric field with respect to the incident flow direction. For the classification scheme applied in the present study, we therefore neglected the impact of the changing latitude of Titan's subsolar point on the draping pattern. However, we subsequently screened the classification results (see column # 7 in Table 3) for a systematic seasonal offset of the polarity reversal layer with respect to our theoretical expectations and found no such tendency.

[44] In a second step, we inspect the observed $B_X$ signature for superimposed disruptions which cannot be explained in terms of draping $\underline{B}_0$ around Titan's ionosphere. Such additional distortions may arise, e.g., from magnetic field fossilization [*Neubauer et al*., 2006; *Bertucci et al*., 2008]. We discriminate between three categories: "weak" means that the magnitude and the spatial extension of these additional $B_X$ perturbations are negligible compared to the primary draping signal, i.e., their extension remains below 10 % and their magnitude below 50 % of the draping signature. The classification "moderate" implies that their magnitude or extension reach up to 75 % of the primary draping signature (which can nonetheless still be identified). In the third category—"strong"—the MAG detected a perturbation signature which is clearly related to Titan's plasma interaction (i.e., its magnitude near C/A clearly exceeds that of the ambient magnetospheric distortions), but its structure is not compatible at all with the idealized picture of field line draping.

[45] In this way, we obtain two labels (↑/ ↓ and weak/moderate/strong) for the draping signatures seen during each Titan flyby. According to the scheme provided in Table 2, each Titan encounter is then assigned to one of the three categories "+", "(+)", or "0."

[46] We would like to note that our classification scheme is based on the observed $B_X$ perturbations only, while the perturbations seen in $B_Y$ and $B_Z$ are not considered to identify disruptions of Titan's induced magnetosphere. As can be seen from Figure 2 in *Neubauer et al*. [2006], the $B_Z$ component is not suitable to identify disruptions in the draping pattern, since—depending on the "intensity" of the draping effect—regions of both $B_Z > 0$ and $B_Z < 0$ may be found in both magnetic hemispheres of Titan. For instance, along the field lines # 3 and # 6 in Figure 2 of *Neubauer et al*. [2006], $B_Z$ continuously remains negative. However, the strongly draped field lines # 4 and # 5 reveal segments with both signs of $B_Z$. Sophisticated numerical modeling for each specific flyby scenario would be required to formulate clear expectations on the locations of regions with negative and positive $B_Z$.

[47] Regarding the $B_Y$ component, one would expect the field lines to be "bulged" in the vicinity of Titan [*Simon et al*., 2009b, Figure 1(ii)]. Such an effect produces a negative sign of $B_Y$ in the $(Y < 0, Z > 0)$ as well as the $(Y > 0, Z < 0)$ sector, whereas perturbations with $B_Y > 0$ should occur in the $(Y < 0, Z < 0)$ and the $(Y > 0, Z > 0)$ sector. However, there is so far not a single Titan flyby which fully matches this very simple theoretical picture. For instance, MAG data from TA (cf. Figure 3 in *Neubauer et al*. [2006]) reveal pronounced $B_Y < 0$ perturbations in the $(Y > 0, Z > 0)$ sector, while observations from TB (cf. Figure 4 in *Neubauer et al*. [2006]) contain long segments of $B_Y > 0$ in the $(Y < 0, Z > 0)$ sector. The occurrence of these signatures does not necessarily point towards a disruption of Titan's induced magnetosphere that is caused by fluctuations of the ambient plasma parameters and fields. Due to the Hall effect and the large gyroradii of newly generated pick-up ions, the Titan interaction region features a pronounced asymmetry between the Saturn-facing and the Saturn-averted hemisphere, leaving a clear imprint in the $B_Y$ pattern and generating regions of $B_Y > 0$/ $B_Y < 0$ in the "wrong" quadrants [*Simon et al*., 2007a, Figures 10c and 13c; and *Simon and Motschmann*, 2009, Figure 3c]. In analogy to $B_Z$, it is therefore not possible to formulate rigid quantitative expectations on the sign of $B_Y$ for an arbitrary flyby scenario.

[48] We would like to emphasize that in this study, we apply a *static* DRAP system and not the *dynamic* coordinate frame introduced by *Neubauer et al*. [2006]. Our intention is to explore how well—despite all the variability—the magnetic field observations from the Titan flybys can still be understood in terms of the idealized pre-Cassini picture, assuming the background magnetic field to be constant on the length and time scales of the plasma interaction. This allows to determine the "robustness" of Titan's induced magnetosphere against ambient field inhomogeneities or fluctuations. We therefore need to compute an average background field from MAG data outside the interaction region and apply it to define a static DRAP system. We can then identify deviations in the structure of the observed interaction signatures from the "prototypical" interaction scenario that would be expected for the constant upstream field defining the DRAP system. In other words, our purpose is to identify the Titan flybys for which spatial and/or temporal variability in the ambient magnetic field conditions can be neglected when attempting to understand the observations made within the moon's induced magnetosphere.

[49] As will be demonstrated later on, Titan's induced magnetosphere has shown to possess a high level of "robustness" against fluctuations/inhomogeneities in the ambient field conditions. The notion of averaging over any kind of ambient field inhomogeneity and interpreting the interaction signatures in terms of a (spatially and temporally) constant background field still seems to be applicable when the fluctuation level in the ambient field is not too high. Thus, we

**Table 3.** Classification of the Magnetic Field Perturbations Observed Within Titan's Induced Magnetosphere During Cassini Flybys TA–T85[a]

| Flyby | Date | SLT | C/A Alt. [km] | Ambient Field | Induced Magnetosph. | Sign($B_X$) | Add.PerturbPoint | Class. |
|---|---|---|---|---|---|---|---|---|
| TA | 26 Oct 2004 | 10.6 | 1174.1 | $Sh - L^S_{Sh}$ | bipolar | ↑ | weak | + |
| TB | 13 Dec 2004 | 10.5 | 1192.3 | $Sh - L^S_{Sh}$ | bipolar | ↑ | moderate | (+) |
| T3 | 15 Feb 2005 | 10.3 | 1579.0 | $L^S_{Sh} - Sh$ | bipolar | ↑ | moderate | (+) |
| T4 | 31 Mar 2005 | 5.3 | 2403.6 | $L^S_{Sh} - L^S_{Sh}$ | Northern lobe | ↑ | moderate | (+) |
| T5 | 16 Apr 2005 | 5.3 | 1026.5 | $Sh - L^S_{Sh}$ | bipolar | ↓ | weak | (+) |
| T6 | 22 Aug 2005 | 5.0 | 3785.3 | $L^S_{Sh} - L^S_{Sh}$ | Southern lobe | ↓ | weak | (+) |
| T7 | 07 Sep 2005 | 5.0 | 2875.3 | | | | | –data gap– |
| T8 | 28 Oct 2005 | 9.3 | 2082.7 | $L^S_{Sh} - L^S_{Sh}$ | Northern lobe | ↑ | weak | + |
| T9 | 26 Dec 2005 | 3.0 | 10,410.9 | $(*) - L^S_{Sh}$ | bipolar | ↑ | moderate | (+) |
| T10 | 15 Jan 2006 | 8.5 | 2042.8 | $L^S_{Sh} - Sh$ | not clear | ? | strong | 0 |
| T11 | 27 Feb 2006 | 1.1 | 1812.0 | $L^S - L^S$ | bipolar | ↓ | weak | (+) |
| T12 | 19 Mar 2006 | 6.4 | 1949.4 | $L^S_{Sh} - L^S_{Sh}$ | Northern lobe | ↑ | weak | + |
| T13 | 30 Apr 2006 | 23.2 | 1855.7 | $Sh - Sh$ | not clear | ? | strong | 0 |
| T14 | 20 May 2006 | 4.4 | 1879.3 | $L^S_{Sh} - L^S$ | Northern lobe | ↓ | weak | (+) |
| T15 | 02 Jul 2006 | 21.2 | 1905.9 | $Sh - Sh$ | Northern lobe | ↓ | weak | (+) |
| T16 | 22 Jul 2006 | 2.4 | 949.9 | $(*) - L^S_{Sh}$ | not clear | ? | strong | 0 |
| T17 | 07 Sep 2006 | 2.3 | 999.5 | $Sh - L^S$ | bipolar | ↓ | weak | (+) |
| T18 | 23 Sep 2006 | 2.3 | 959.8 | $L^S - L^S_{Sh}$ | bipolar | ↑ | weak | + |
| T19 | 09 Oct 2006 | 2.2 | 979.7 | $L^S_{Sh} - Sh$ | bipolar | ↓ | weak | (+) |
| T20 | 25 Oct 2006 | 2.2 | 1029.5 | $Sh - L^S$ | bipolar | ↓ | weak | (+) |
| T21 | 12 Dec 2006 | 2.1 | 1000.0 | $L^S_{Sh} - L^S$ | bipolar | ↓ | moderate | 0 |
| T22 | 28 Dec 2006 | 2.0 | 1296.8 | $L^S - Sh$ | bipolar | ↓ | moderate | 0 |
| T23 | 13 Jan 2007 | 2.0 | 1000.3 | $(*) - L^S$ | not clear | ? | strong | 0 |
| T24 | 29 Jan 2007 | 1.9 | 2631.2 | $Sh - L^S_{Sh}$ | Southern lobe | ↑ | moderate | (+) |
| T25 | 22 Feb 2007 | 13.9 | 1000.4 | | | | | –data gap– |
| T26 | 10 Mar 2007 | 13.8 | 980.6 | $L^S_{Sh} - Sh$ | bipolar | ↑ | weak | + |
| T27 | 26 Mar 2007 | 13.8 | 1009.9 | $Sh - Sh$ | bipolar | ↑ | moderate | (+) |
| T28 | 10 Apr 2007 | 13.7 | 990.9 | $Sh - Sh$ | Northern lobe | ↑ | moderate | (+) |
| T29 | 26 Apr 2007 | 13.7 | 980.8 | $Sh - Sh$ | bipolar | ↓ | weak | (+) |
| T30 | 12 May 2007 | 13.6 | 959.2 | $Sh - Sh$ | bipolar | ↓ | weak | (+) |
| T31 | 28 May 2007 | 13.6 | 2298.6 | $Sh - Sh$ | Northern lobe | ↑ | weak | + |
| T32 | 13 Jun 2007 | 13.6 | 964.9 | m'sheath | | | | –m'sheath– |
| T33 | 29 Jun 2007 | 13.6 | 1932.6 | $Sh - Sh$ | Northern lobe | ↑ | weak | + |
| T34 | 19 Jul 2007 | 18.8 | 1331.8 | $Sh - Sh$ | bipolar | ↑ | moderate | (+) |
| T35 | 31 Aug 2007 | 11.5 | 3324.2 | $L^S_{Sh} - Sh$ | Northern lobe | ↑ | moderate | (+) |
| T36 | 02 Oct 2007 | 11.5 | 973.0 | $Sh - Sh$ | not clear | ? | strong | 0 |
| T37 | 19 Nov 2007 | 11.4 | 999.4 | | | | | –data gap– |
| T38 | 05 Dec 2007 | 11.4 | 1298.3 | $Sh - Sh$ | Southern lobe | ↑ | moderate | (+) |
| T39 | 20 Dec 2007 | 11.4 | 969.5 | $Sh - Sh$ | not clear | ? | strong | 0 |
| T40 | 05 Jan 2008 | 11.3 | 1014.0 | $(*) - Sh$ | bipolar | ↓ | moderate | 0 |
| T41 | 22 Feb 2008 | 11.2 | 999.7 | $L^S_{Sh} - L^S_{Sh}$ | bipolar | ↑ | moderate | (+) |
| T42 | 25 Mar 2008 | 11.1 | 999.4 | m'sheath | | | | –m'sheath– |
| T43 | 12 May 2008 | 11.0 | 1001.4 | $L^S_{Sh} - L^S_{Sh}$ | bipolar | ↓ | weak | (+) |
| T44 | 28 May 2008 | 10.9 | 1400.0 | $Sh - Sh$ | bipolar | ↓ | moderate | 0 |
| T45 | 31 Jul 2008 | 10.7 | 1613.8 | $L^S_{Sh} - Sh$ | not clear | ? | strong | 0 |
| T46 | 03 Nov 2008 | 10.5 | 1105.2 | $L^S_{Sh} - Sh$ | Southern lobe | ↑ | weak | + |
| T47 | 19 Nov 2008 | 10.4 | 1023.4 | $Sh - Sh$ | Southern lobe | ↓ | weak | (+) |
| T48 | 05 Dec 2008 | 10.4 | 960.6 | $Sh - Sh$ | bipolar | ↑ | weak | + |
| T49 | 21 Dec 2008 | 10.3 | 970.6 | $Sh - Sh$ | bipolar | ↓ | weak | (+) |
| T50 | 07 Feb 2009 | 10.2 | 966.8 | $Sh - Sh$ | not clear | ? | strong | 0 |
| T51 | 27 Mar 2009 | 10.1 | 962.6 | $Sh - Sh$ | bipolar | ↑ | weak | + |
| T52 | 04 Apr 2009 | 22.1 | 4146.6 | oscill. sheet | not clear | ? | strong | [−] |
| T53 | 20 Apr 2009 | 22.0 | 3598.8 | oscill. sheet | Northern lobe | ? | moderate | [(+)] |
| T54 | 05 May 2009 | 22.0 | 3242.4 | oscill. sheet | not clear | ? | strong | [−] |
| T55 | 21 May 2009 | 22.0 | 965.7 | oscill. sheet | Northern lobe | ? | moderate | [(+)] |
| T56 | 06 Jun 2009 | 21.9 | 967.7 | oscill. sheet | not clear | ? | strong | [−] |
| T57 | 22 Jun 2009 | 21.9 | 955.1 | oscill. sheet | bipolar | ? | moderate | [(+)] |
| T58 | 08 Jul 2009 | 21.8 | 965.8 | oscill. sheet | bipolar | ? | strong | [−] |
| T59 | 24 Jul 2009 | 21.8 | 956.2 | oscill. sheet | bipolar | ? | moderate | [(+)] |
| T60 | 09 Aug 2009 | 21.7 | 971.1 | oscill. sheet | bipolar | ? | moderate | [(+)] |
| T61 | 25 Aug 2009 | 21.7 | 960.7 | oscill. sheet | Southern lobe | ? | moderate | [(+)] |
| T62 | 12 Oct 2009 | 21.6 | 1299.5 | oscill. sheet | not clear | ? | strong | [−] |
| T63 | 12 Dec 2009 | 17.0 | 4847.5 | $Sh - Sh$ | not clear | ? | strong | 0 |
| T64 | 28 Dec 2009 | 17.0 | 951.3 | $Sh - Sh$ | | | | –data gap– |
| T65 | 12 Jan 2010 | 16.9 | 1074.0 | oscill. sheet | Southern lobe | | moderate | [(+)] |
| T66 | 28 Jan 2010 | 17.0 | 7486.4 | $Sh - Sh$ | | | | far upstr. |
| T67 | 05 Apr 2010 | 21.1 | 7437.5 | oscill. sheet | | | | far upstr. |
| T68 | 20 May 2010 | 16.1 | 1397.6 | oscill. sheet | Southern lobe | ? | moderate | [(+)] |

(*Continues*)

Table 3. (Continued)

| Flyby | Date | SLT | C/A Alt. [km] | Ambient Field | Induced Magnetosph. | Sign($B_X$) | Add.PerturbPoint | Class. |
|---|---|---|---|---|---|---|---|---|
| T69 | 05 Jun 2010 | 16.1 | 2042.4 | oscill. sheet | Northern lobe | ? | moderate | [(+)] |
| T70 | 21 Jun 2010 | 16.1 | 878.1 | $Sh - Sh$ | Northern lobe | ↑ | weak | + |
| T71 | 07 Jul 2010 | 16.1 | 1003.7 | $Sh - Sh$ | Southern lobe | ↑ | weak | + |
| T72 | 24 Sep 2010 | 16.0 | 8177.7 | $Sh - Sh$ | | | | far upstr. |
| T73 | 11 Nov 2010 | 15.8 | 7925.7 | $Sh - Sh$ | no clear Titan signature | ? | ? | – |
| T74 | 18 Feb 2011 | 20.6 | 3651.1 | $Sh - Sh$ | | | | far upstr. |
| T75 | 19 Apr 2011 | 14.2 | 10,052.9 | $Sh - Sh$ | no clear Titan signature | ? | ? | – |
| T76 | 08 May 2011 | 19.8 | 1872.7 | oscill. sheet | not clear | ? | strong | [−] |
| T77 | 20 Jun 2011 | 12.2 | 1358.8 | $Sh - Sh$ | Southern lobe | ↑ | weak | + |
| T78 | 12 Sep 2011 | 17.5 | 5821.4 | $Sh - Sh$ | Southern lobe | ↓ | moderate | 0 |
| T79 | 13 Dec 2011 | 12.9 | 3583.0 | $L^N_{Sh} - Sh$ | | | | far upstr. |
| T80 | 02 Jan 2012 | 18.6 | 29,513.7 | oscill. sheet | | | | far upstr. |
| T81 | 30 Jan 2012 | 12.6 | 31,130.1 | $L^N_{Sh} - Sh$ | | | | far downstr. |
| T82 | 19 Feb 2012 | 18.4 | 3803.0 | oscill. sheet | not clear | ? | strong | [−] |
| T83 | 22 May 2012 | 13.7 | 955.0 | $Sh - L^N_{Sh}$ | not clear | ? | strong | 0 |
| T84 | 07 Jun 2012 | 13.7 | 959.0 | $Sh - Sh$ | bipolar | ↓ | moderate | 0 |
| T85 | 24 Jul 2012 | 13.6 | 1012.0 | m'sheath | | | | –m'sheath– |

[a]The first column provides the flyby number, whereas the date of C/A, Titan's orbital position (SLT), and the altitude of C/A are listed in the second, third, and fourth column, Respectively. In the fifth column, we characterize the ambient magnetospheric field conditions inbound and outbound of C/A, with the symbol on the L.H.S. of the dash referring to the inbound region and the symbol on its R.H.S. characterizing the outbound region. This classification of the ambient field conditions has been adopted from Table 5 in *Simon et al*. [2010a] and Table 1 in the present study. The sixth column indicates which segment of Titan's induced magnetosphere was sampled during the encounter. The term "bipolar" implies that Cassini intersected both, the moon's northern (negative $B_X$ perturbation) and the southern (positive $B_X$ perturbation) magnetic hemisphere. The last three columns contain the classification of Titan's induced magnetosphere according to the criteria introduced in Section 3.2: Sign of $B_X$ (column #7), magnitude of additional perturbations that disrupt the draping pattern (column #8) and classification obtained from Table 2 (column #9). The asterisk symbol appearing in the fifth column refers to regions where a discrimination between signatures of Titan's local interaction and ambient magnetospheric fluctuations was not possible (cf. *Simon et al*. [2010a] for details). encounters T32, T42, and T85 occurred when Titan was located in saturn's magnetosheath ("m'sheath").

intend to demonstrate that the pre-Cassini picture of the Titan interaction (treating the background field as constant) is far better applicable than one might expect in light of the high level of observed ambient variability. A similar static coordinate frame has also been applied by *Bertucci et al*. [2007] for T9 and by *Ulusen et al*. [2012] to study flyby data that were collected under perturbed current sheet conditions.

[50] In the case of Titan being exposed to strong north-south oscillations of the current sheet with different signs of $B_{0,x}$ and $B_{0,y}$ on both sides of C/A, the notion of an interaction with a constant magnetospheric background field is certainly not applicable. Nonetheless, we can still screen the magnetic field observations around C/A for clearly discernable signatures of Titan's induced magnetosphere. As shown by *Simon et al*. [2010a], even during strong current sheet oscillations, only the polarities of $B_x$ and $B_y$ (in TIIS coordinates) near Titan's orbit undergo changes, while $B_z$ retains its negative sign. For this reason, one would still expect the formation of a draping pattern with negative $B_x$ perturbations in Titan's northern hemisphere and positive $B_x$ perturbations in the moon's southern hemisphere.

[51] However, the location of the boundary between the two $B_x$ polarity regimes is not well defined any more. Only very few modeling studies have so far focused on the magnetic field configuration near Titan under nonstationary magnetospheric upstream conditions [*Simon et al*., 2008a, 2009a; *Simon and Motschmann*, 2009]. Unfortunately, all these studies included strong simplifications of the incident magnetic field conditions and mainly focused on the qualitative physics of Titan's induced magnetosphere in a time-dependent environment. For this reason, we cannot apply modeling results to determine how strong Titan's induced magnetosphere differs from an idealized, time-dependent "prototype."

[52] Therefore, we need to apply a far less rigid scheme to classify the magnetic field observations from these encounters (T52–T62, T65, T68, T69, T76, T82, see Table 3) and drop our criterion for the location of the polarity reversal layer. Instead, we search the $\pm 1.5$ h interval around C/A for a clearly discernable Titan interaction signature and compare its magnitude to that of the ambient current sheet oscillations. The label "weak" then means that the magnitude of the draping signature in $B_x$ exceeds that of the ambient $B_x$ perturbations by at least a factor of 5, while "moderate" means that it is only about a factor of 2 larger. In the "strong" case, the magnitude of the $B_x$ perturbations around C/A is comparable to or even exceeded by the ambient magnetospheric perturbations. In the latter case, the $B_x$ distortions seen at C/A cannot be clearly ascribed to Titan's magnetospheric interaction, but they may also arise from ambient magnetospheric fluctuations which occurred coincidentally. Thus, an unambiguous identification of Titan's induced magnetosphere in MAG data is not possible. The flybys of the "oscillatory sheet" category will receive a separate treatment in our discussion of the classification results. For these flybys, we apply the classification symbols "[+]" (corresponding to weak ambient perturbations), "[(+)]" (moderate), and "[−]" (strong).

[53] In the following section, we shall present a series of examples, illustrating how the above classification criteria are applied to specific flyby scenarios.

## 4. Classification Scheme: Examples

[54] In this section, we will elaborate on the application of our classification scheme to selected Titan flybys. The classification results for these encounters are also listed in Table 3.

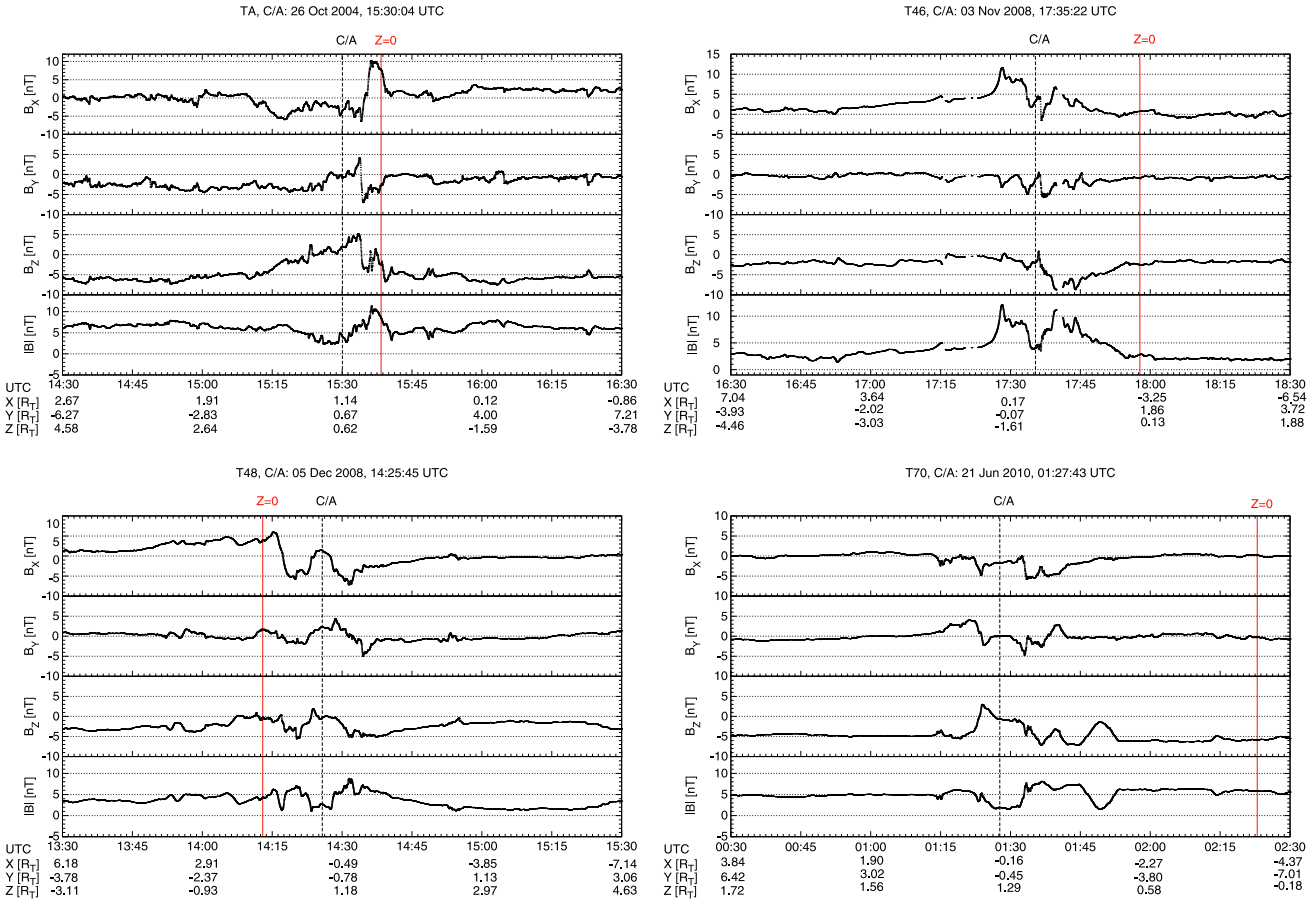


**Figure 3.** Cassini magnetic field observations from Titan flybys TA, T46, T48, and T70, displayed in DRAP coordinates (ideal draping category, "+"). In each plot, the position of closest approach (C/A) is denoted by the vertical dashed line. The red line indicates Cassini's passage through the ($Z=0$) plane of the DRAP coordinate system. The ambient field conditions during these flybys were assigned to the *Sh–L* (TA), the *L–Sh* (T46), and the *Sh–Sh* (T48, T70) category, respectively.

### 4.1. Ideal Draping Pattern (Category "+")

[55] Figure 3 displays Cassini magnetic field observations in DRAP coordinates for Titan flybys TA, T46, T48, and T70, which have all been assigned to the "+" category.

[56] As can be seen from Table 5 in *Simon et al*. [2010a], TA belongs to the "$Sh - L^{S}_{Sh}$" category, i.e., the southern lobe-type field detected outbound of Titan has been applied to define the DRAP coordinate system. The background value $B_{0,X}$ is nearly zero in the inbound region (*Sh* regime), whereas the sweepback of the field lines [*Bertucci et al*., 2009] generates a positive $B_{0,X}$ in the outbound region. As expected, the $B_{0,Y}$ component nearly vanishes outbound of Titan, since the background field for the definition of the DRAP system was obtained from that region.

[57] Let us now have a look at the Titan interaction signature detected in $B_X$ around C/A (cf. upper left panel in Figure 3). During TA, Cassini crossed the ($Z=0$) plane of the DRAP system steep from north to south. Therefore, the MAG detected a bipolar perturbation in $B_X$: the passage through Titan's northern lobe ($B_X<0$, 15:10–15:35) is followed by a positive $B_X$ perturbation after 15:35, indicative of Titan's southern lobe. The slight reduction in the magnitude of the $B_X$ perturbation between 15:20 and 15:30 coincides with a decrease of $|B|$, i.e., it indicates Cassini's passage through the magnetic ionopause region where the field is shielded by Titan's ionosphere (see also *Neubauer et al*. [2006]). Figure 3 also shows that the polarity reversal layer was crossed in the ($X>0, Z>0$) half space, which is consistent with Figure 2b. Intersection of the polarity reversal layer occurred at ($X=0.9R_T, Z=0.2R_T$). Since the background field components (in DRAP coordinates) read $B_{0,X}\approx+2$nT and $B_{0,Z}\approx-6$nT, the layer was crossed below the $Z=|\frac{B_{0,X}}{B_{0,Z}}|X$ plane, which is again consistent with theoretical expectations.

[58] In agreement with the analysis of *Neubauer et al*., [2006], we find that no noteworthy disruption signatures are superimposed on the draping pattern observed during TA. Thus, the two labels of this flyby are "↑" (correct location of polarity reversal layer) and "weak" for the magnitude of superimposed perturbations which cannot be explained in terms of the draping picture. According to Table 2, the TA flyby is therefore classified as "+," i.e., Titan's induced magnetosphere exhibits a well-defined draping pattern.

[59] Another flyby of the "+" category is T46. As can be seen from the upper right panel in Figure 3, Cassini passed only through Titan's southern magnetic lobe while being located in the ($Z<0$) half space. The $B_X$ component outside the Titan interaction region is negligible, implying that this

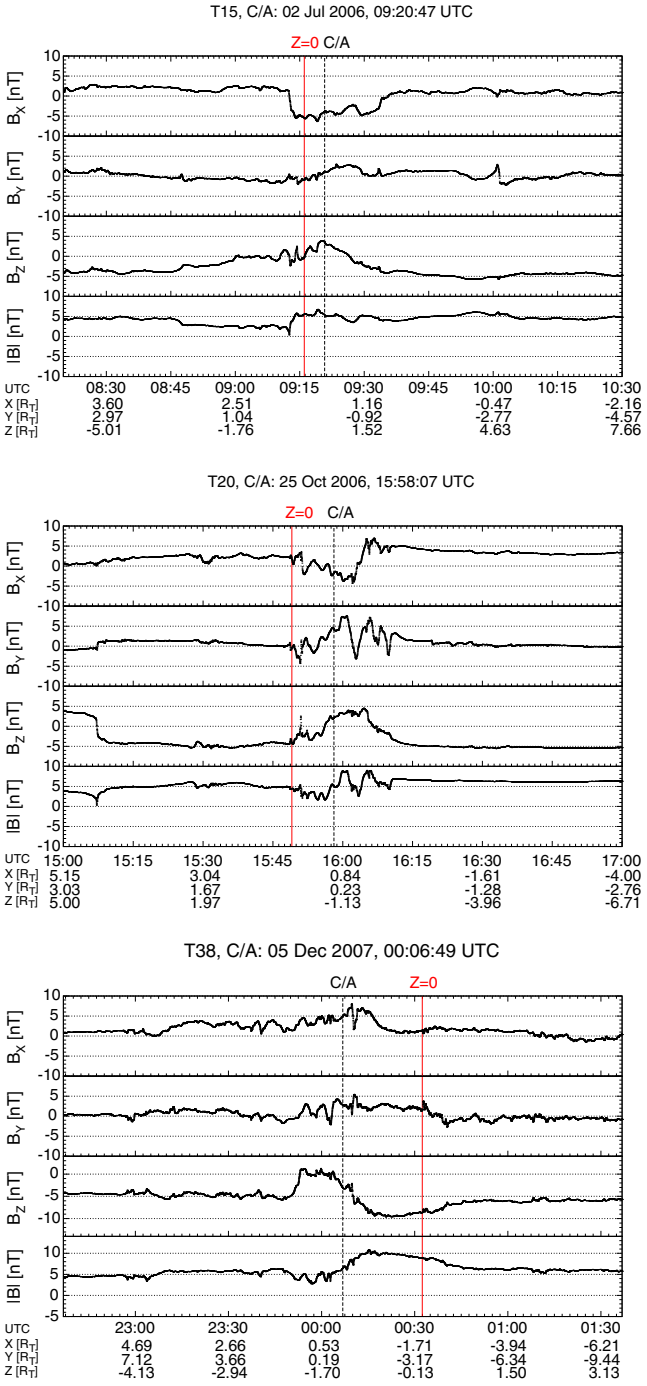


**Figure 4.** Cassini magnetic field observations from Titan flybys T15, T20, and T38 (moderately perturbed draping pattern, "(+)"), displayed in DRAP coordinates. The ambient field conditions during these flybys were assigned to the *Sh–L* (T20) and the *Sh–Sh* (T15, T38) category, respectively.

flyby corresponds to scenario (a) in Figure 2. Thus, the location of the observed $B_X$ perturbations is in agreement with theoretical expectations ("↑"). Similar to TA, the MAG detected a decrease of both the $B_X$ enhancement and the total field strength in a short interval around C/A (between 17:30 and 17:40), indicative of Cassini's passage near Titan's magnetic ionopause. Besides, the $B_X$ component observed during T46 does not reveal any noteworthy perturbations which cannot be explained in terms of the draping picture.

[60] The T48 encounter is another flyby during which the MAG detected a bipolar $B_X$ perturbation, along with a passage near Titan's magnetic ionopause around C/A (see lower left panel in Figure 3). During this encounter, Cassini crossed the Titan interaction region from ($Z<0$) to ($Z>0$), i.e., the spacecraft first penetrated the southern magnetic lobe ($B_X>0$), followed by a passage through Titan's northern magnetic hemisphere ($B_X<0$). The transition from southern to northern magnetic polarity was encountered in the ($X>0, Z>0$) sector and only about 0.2 $R_T$ above the ($Z=0$) plane. The slight tilt of the polarity reversal layer into the ($Z>0$) half space arises from the positive $B_{0,X}$ component in the inbound region. The intersection occurred at $X=1.1\ R_T$, i.e., below the $Z=|\frac{B_{0,X}}{B_{0,Z}}|X$ plane (background field components $B_{0,X}\approx 1$ nT, $B_{0,Z}=-2.5$ nT). Thus, the observed magnetic polarity is again consistent with theoretical expectations ("↑"). Again, the draping signature (outside the magnetic ionopause region) is not obscured by any significant disruptions. Hence, T48 was assigned to the "+" category.

[61] Finally, let us have a look at Cassini MAG data from the T70 encounter, cf. lower right panel in Figure 3. During the entire Cassini mission, no other Titan flyby is scheduled to achieve such a small C/A altitude (878.1 km). As discussed in section 2, T70 is also the encounter during which the ambient magnetic field conditions were in best agreement with the idealized picture from the pre-Cassini era. During T70, Cassini remained north of Titan ($Z>0$) along the entire passage through the interaction region. Consequently, the MAG detected only a negative $B_X$ perturbation. Again, the decrease of the $B_X$ perturbation near C/A is accompanied by a reduction of $|\underline{B}|$, indicative of a passage near the magnetic ionopause [*Neubauer et al.*, 2006]. Only the tiny spike in $B_X$ observed at about 01:36 cannot be explained in terms of steady-state draping. However, this structure is weak compared to the extent and magnitude of the primary perturbation signal in $B_X$. Thus, T70 meets both criteria for an "ideal" draping signature and is assigned to the "+" category.

[62] The combination of a nearly southward, quiet background field with an unperturbed induced magnetosphere makes T70 the only Titan encounter to date which completely matches the picture frequently studied in pre-Cassini models of the Titan interaction (see, e.g., *Kallio et al.* [2004]; *Ledvina et al.* [2004]). Even the background field $\underline{B}_0=(0,0,-5)$nT (valid in DRAP *and* TIIS coordinates) quantitatively matches the value applied in numerous models of the Titan interaction.

### 4.2. Moderately Perturbed Draping Signature (Category "(+)")

[63] In this subsection, we present three examples of flybys with noticeable deviations from the steady-state draping picture, namely T15, T20, and T38.

[64] The upper panel in Figure 4 displays MAG data from the T15 encounter. As can be seen, Cassini passed only through Titan's northern lobe ($B_X<0$) during this flyby, with the interaction signature observed clearly downstream of Titan ($X>0$). The $B_{0,X}$ component of the ambient field

outside the interaction region is slightly positive inbound and outbound, i.e., one would expect Titan's northern lobe to be confined to the ($Z > 0$) half space. Nonetheless, the spacecraft detected the onset of the ($B_X < 0$) perturbation while still located in the ($Z < 0$) half space, which is incompatible with the magnetic field pattern shown in Figure 2b. On the other hand, only weak disruptions are superimposed on the primary draping signal around 09:26. According to Table 2, T15 is therefore assigned to the "(+)" category.

[65] Another flyby of the same type is T20, as shown in the middle panel of Figure 4. During this encounter, Cassini passed through both magnetic lobes, with the perturbation signatures completely located in the ($X > 0$) half space. However, although this flyby occurred in southern summer and $B_{0,X}$ was therefore slightly positive, the signatures of both magnetic lobes and the polarity reversal layer in between them are shifted in the ($Z < 0$) half space, which is at variance with Figure 2b. Nevertheless, the Titan interaction signature is again clearly discernable in the magnetic field data. The slight reduction in the magnitude of the $B_X$ perturbation about five minutes before C/A coincides with a decrease in the total field strength, i.e., it is indicative of Cassini approaching Titan's magnetic ionopause.

[66] Regarding the background magnetospheric field conditions during T20, *Simon et al*. [2010a]showed that the MAG detected a region of highly perturbed current sheet fields in the inbound region, which abruptly ended about one hour before C/A (see Figure 6 in that work). In the outbound segment of T20, the MAG subsequently observed a remarkably quiet lobe-type regime which has been applied to compute the background field for the transformation to the DRAP system. Despite the highly perturbed field conditions on one side of C/A, the structure of Titan's induced magnetosphere is still in good agreement with the draping picture. MAG data from T20 therefore imply that the "shaking" of Titan's induced magnetosphere by the inbound current sheet motion only leads to a displacement of the magnetic lobes, but it does not cause a disruption of the expected interaction signature beyond recognition.

[67] For both T15 and T20, a stationary upstream flow that was tilted with respect to the corotation direction might provide another explanation for the shifted location of the polarity reversal layer.

[68] The lower panel of Figure 4 displays the magnetic field perturbations detected during T38 when the spacecraft passed through Titan's southern magnetic lobe. Cassini entered the interaction region at about 23:10 and left it around 00:30. Outside the interaction region, the $B_X$ component is exceeded by $B_Z$ by more than a factor of 5 (cf. interval between 22:30 and 23:00), i.e., one would expect the polarity reversal layer to coincide with the ($Z = 0$) plane. In agreement with this picture, the positive $B_X$ perturbations detected by Cassini are well confined to the ($Z < 0$) half space. However, MAG data also reveal several superimposed distortions which partially obscure the primary draping signal: between 23:40 and 23:50, the $B_X$ perturbation decreased by more than a factor of three. Another spikey dip was detected shortly after C/A at about 00:10. Since the draping picture does not provide a straightforward explanation for any of these signatures, the superimposed distortions seen during T38 are classified as "moderate" and—despite the correct location of the $B_X > 0$ region—the encounter is assigned to the "(+)" category.

### 4.3. Strongly Perturbed Interaction Region (Category "0")

[69] Although the MAG observed a clearly discernable Titan interaction signature during the three flybys discussed in this section—T36, T39, and T44—MAG data from none of them can be explained in terms of the steady-state draping picture.

[70] The upper panel of Figure 5 displays the interaction signature observed by Cassini during the T36 flyby while located downstream of Titan ($X > 0$) and in the ($Z < 0$) half space. When entering the interaction region at about 04:25, the MAG instrument detected a steady enhancement of $B_X$, indicative of Titan's southern magnetic lobe. Since $B_{0,X}$ is slightly positive outside the interaction region, this observation is in agreement with Figure 2b. Subsequently, the spacecraft observed two dips in $B_X$ at about 04:38 and 04:43, both of them accompanied by a decrease of the total field strength. In between these two signatures, the $B_X$ enhancement nearly returned to its initial value above $B_X = 5$nT. If both dips correspond to passages near Titan's magnetic ionopause, these data indicate a highly inhomogeneous and/or dynamic structure of this boundary layer, which is not reproduced by numerical simulations [*Backes*, 2005]. However, the most remarkable feature of the T36 observations is a complete reversal of the $B_X$ polarity shortly after C/A. The peak field strength achieved at the bottom of this dip is on the order of $B_X = -12$nT, i.e., it denotes the by far strongest distortion of Saturn's magnetic field during the T36 flyby. Before leaving the interaction region, Cassini again observed magnetic fields of southern lobe polarity. Since neither the multiple decreases of $B_X$ before and at C/A nor the strong "antidraping" signature—constituting the predominant feature of the T36 interaction region—can be explained in terms of simple field line draping, T36 has been assigned to the "0" category.

[71] An even stronger disrupted interaction signature has been detected during T39, as displayed in the middle panel of Figure 5. Since the $B_{0,X}$ component was nearly zero on both sides of C/A and the spacecraft passed through the near-Titan region in the ($Z < 0$) half space, Cassini should only have intersected Titan's southern lobe ($B_X > 0$, cf. Figure 2a). However, the primary draping signal is interrupted by a broad region of reversed draping polarity between 22:50 and 23:05, which is flanked by a discontinuity-like decrease of $B_X$ on either side ($\delta B_X = -15 \ldots -20$ nT). The peak perturbation of $\delta B_X = -10$ nT achieved in the outbound region near 23:03 is comparable to the magnitude of the "correct" draping signatures at both flanks of the valley. In analogy to T36, the T39 encounter therefore belongs to the "0" category.

[72] Although the disruptions of the draping pattern seen along the trajectory of T44 are weaker than during T36 and T39, the flyby is assigned to the "0" category as well (cf. lower panel in Figure 5). During T44 Cassini intersected both, the southern and the northern magnetic lobe, with the interaction region embedded in highly perturbed current sheet fields (*Sh*–*Sh*) on both sides. The spacecraft entered Titan's southern lobe ($B_X > 0$) at about 07:05 and then crossed the polarity reversal layer around 08:10.

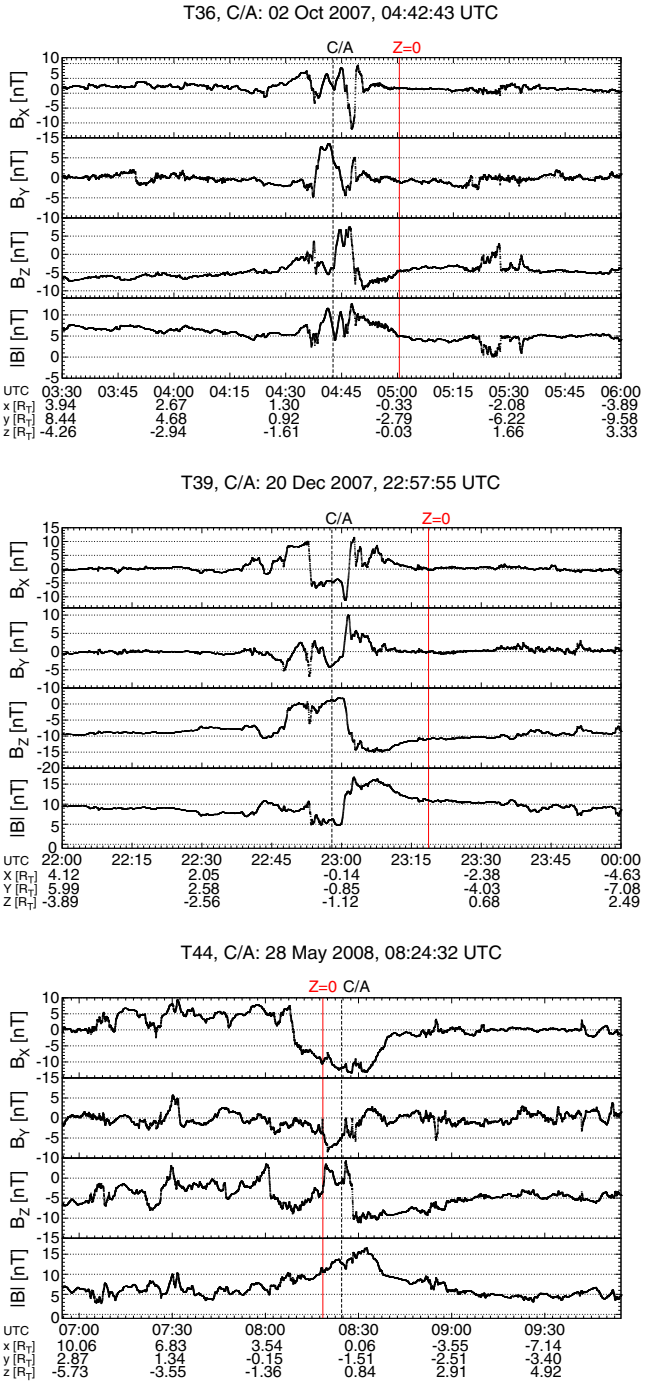


**Figure 5.** Cassini magnetic field observations from Titan flybys T36, T39, and T44 (strongly perturbed interaction region, "0"), displayed in DRAP coordinates. The ambient field conditions during these three flybys were assigned to the *Sh–Sh* category.

Subsequently, Cassini left the interaction region at about 08:40. As can be seen from Figure 5, the field fluctuations caused by the motion of Saturn's current sheet have left a clear imprint in Titan's northern magnetic lobe, revealing several regions where the draping signature almost vanishes. The impact of the ambient field disruptions on the draping pattern is therefore classified as "moderate." The disruptions of the near-Titan region by Saturn's current sheet are also well visible in $B_Y$ and $B_Z$. We note that the impact of ambient field fluctuations on the visibility of the draping pattern is less pronounced in the northern magnetic lobe. Although the background $B_{0,X}$ component is nearly zero on both sides of the interaction region, the polarity reversal layer is clearly shifted in the ($Z < 0$) hemisphere, at variance with Figure 2a ("↓"). According to Table 2, T44 is therefore assigned to the "0" category.

[73] One might argue that flybys of the "↓/moderate" type—like T44—should rather be assigned to the "(+)" than the "0" category, since the interaction signature still permits an identification of the draping pattern. However, as can be seen from Table 3, the available dataset encompasses only six encounters of this type: while T22 belongs to the *L–Sh* category, Cassini detected current sheet fields on both sides of C/A during T40, T44, T78, and T84. The T21 encounter occurred with Titan embedded in the southern lobe of Saturn's magnetodisk. As can be seen from Table 4, moving these encounters from the "0" to the "(+)" category does not impose any changes at all on the overall picture obtained from the classification.

### 4.4. No Discernable Titan Interaction Signature (Category "-")

[74] An example of this category is the T54 encounter, the magnetic field observations of which are displayed in Figure 8 of *Simon et al*. [2010a]. As can be seen from the $B_x$ signature, C/A to Titan coincided with a sweep of Saturn's current sheet through the interaction region, going along with a reversal in the polarities of the $B_x$ and $B_y$ components. Although MAG data reveal a tiny dip in $B_x$ near C/A, the magnitude of this signature is clearly exceeded by that of the $B_x$ polarity reversal associated with ambient current sheet motion. Especially, MAG data acquired during the subsequent crossing of Saturn's current sheet between 02:00 and 04:00 indicate that such a short-scale "jitter" of $B_x$ may well arise from current sheet dynamics and cannot be clearly ascribed to Titan's induced magnetosphere. The T54 flyby is therefore assigned to the "[−]" category, indicating that an unambiguous discrimination between the Titan interaction region and external magnetospheric dynamics is not possible.

[75] Another encounter of the same category is T56 (see Figure 6). During T56, C/A to Titan again coincided with a sweep of Saturn's current sheet through the interaction region from north to south, going along with a reversal in the signs of both, $B_x$ and $B_y$. C/A of T56 occurred only about an hour after the orientation of $B_x$ and $B_y$ had started to change. A few minutes after C/A, the MAG detected a sudden enhancement in both components, lasting until about 21:00. However, the peak values achieved by both components between C/A and 21:00 are comparable to the background level of $B_x$ and $B_y$ in the inbound region (between 17:00 and 19:00) where Cassini was still embedded in the southern magnetodisk lobe regime. For this reason, it is not possible to unambiguously ascribe the $B_x$ enhancement seen after C/A to the Titan interaction. This structure might also arise from the large-scale dynamics of Saturn's current sheet, the sweeps of which through Titan's orbital plane are frequently accompanied by some "jitter" in $B_x$

**Table 4.** Structure of Titan's Induced Magnetosphere: Dependence on Ambient Magnetic Field Conditions[a]

| | + | (+) | 0 | - |
|---|---|---|---|---|
| *L – L* | T8, T12, T18 | T4, T6, T11, T14, T41, T43 | T21 | none |
| *L – Sh* / *Sh – L* | TA, T26, T46 | TB, T3, T5, T9, T17, T19, T20, T24, T35 | T10, T16, T22, T23, T45, T83 | none |
| *Sh – Sh* | T31, T33, T48, T51, T70, T71, T77 | T15, T27, T28, T29, T30, T34, T38, T47, T49 | T13, T36, T39, T40, T44, T50, T63, T78, T84 | T73, T75 |
| oscill. sheet | none | T53, T55, T57, T59, T60, T61, T65, T68, T69 | –not applicable– | T52, T54, T56, T58, T62, T76, T82 |

[a]The table illustrates the correlation between our classification of Titan's induced magnetosphere (+, (+), 0, −) and the magnetic field conditions around C/A. In this table, the symbol "*L–L*" refers to Titan flybys during which lobe-type fields *of the same polarity* were observed on both sides of C/A, whereas "*L–Sh*" and "*Sh–L*" denote encounters during which lobe-type fields were observed only inbound *or* outbound of Titan, respectively. The few flybys for which a discrimination between Titan interaction signatures and ambient magnetospheric perturbations was not possible on one side of C/A (asterisk in Table 3) are assigned to this category as well, since the background field in both cases is computed from data collected only on *one* side of C/A. During encounters of the "*Sh–Sh*" category, Titan was embedded in current sheet fields on both sides of C/A. Encounters that coincided with a sweep of saturn's current sheet through the local interaction region are listed in the bottom row ("oscill. sheet"). For encounters of the "oscill. sheet" category, the classification symbols "+," "0," and "−" need to be replaced by their less rigid counterparts "[+]," "[0]," and "[−]," respectively.

and $B_y$ instead of a steady transition (see also *Arridge et al.* [2008a]).

## 5. Titan's Induced Magnetosphere During Flybys TA–T85

[76] The classification technique introduced in sections 3.2 and 4 has been applied to Cassini MAG data from the available Titan flybys between Saturn Orbit Insertion (July 2004) and the initial submission date of this publication (fall 2012, TA–T85). The results of this classification are provided in Table 3. In Table 4, we put the field signatures seen within the Titan interaction region in relation to the ambient magnetospheric field conditions around C/A. Figure 7 displays the distribution of Titan flybys with a strongly disrupted interaction region (categories "0" and "-," denoted in red) on the various local time sectors, while the relation between these flybys and their C/A altitudes can be seen in Figure 8. We would like to note that for the generation of Figures 7 and 8, we have not considered the 18 Titan encounters from the "oscillatory sheet" category for which a far less rigid classification scheme was applied.

[77] It is interesting to note that although MAG data from 85 Titan flybys were available at the time of this writing, numerous of them are not suitable for a characterization of Titan's magnetospheric interaction: during 16 flybys, the $B_x$ and $B_y$ components of the background field reversed their polarities while Cassini was located within the Titan interaction region, i.e., any Titan-related signatures were to a high degree "contaminated" by ambient magnetospheric fluctuations of large amplitude. During another seven flybys, Titan was either located outside the magnetosphere of Saturn at the time of C/A, or large data gaps prevented an analysis of the interaction region. C/A of another seven encounters occurred at such a large distance to the moon that—based on modeling results [*Simon et al.*, 2007a; *Ma et al.*, 2006]—one would not expect to observe any measurable signatures of the Titan interaction. Thus, at the time of this writing, only 55 Titan flybys were left for an application of our classification scheme. By the scheduled end of the Cassini mission in 2017, the spacecraft will hopefully have accomplished a total number of 126 Titan flybys, i.e., about 40 additional encounters should then be available to complete our picture of Titan's magnetospheric interaction. However, we do not expect these additional flybys to drastically alter the picture derived in the present study, especially when assuming that again, one third of the encounters will not be suitable for the analysis method we propose.

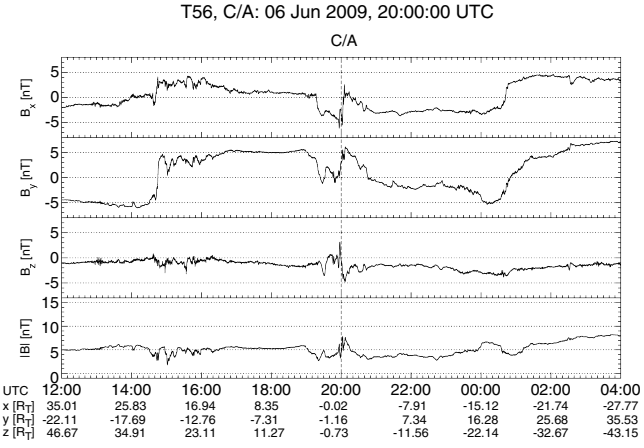


**Figure 6.** Cassini magnetic field observations within a ± 8 h interval around C/A of Titan flyby T56, displayed in TIIS coordinates.

## 6. Discussion of Classification Results

[78] Table 4 shows the distribution of Titan flybys with different ambient magnetic field conditions on the various classification categories. So far, quiet lobe-type fields within a ± 3 h window around C/A were observed during only 10 Titan flybys of the entire Cassini mission (see row "*L–L*" in Table 4). As expected, the structure of Titan's induced magnetosphere is then well described by the stationary draping picture: nine out of ten flybys of the "*L–L*" type are assigned to either the "+" or the "(+)" category. Regarding the six flybys of the "(+)" category (T4, T6, T11, T14, T41, and T43), the additional field disruptions observed during T41 may arise from field fossilization due to weak current sheet intrusions into the near-Titan region, as observed in the inbound and outbound regions [*Simon et al.*, 2010a, Table 5]. On the other hand, the nearly unperturbed, but slightly shifted draping signals detected during T11, T14, and T43 (labels "↓" and "weak") possibly indicate that the

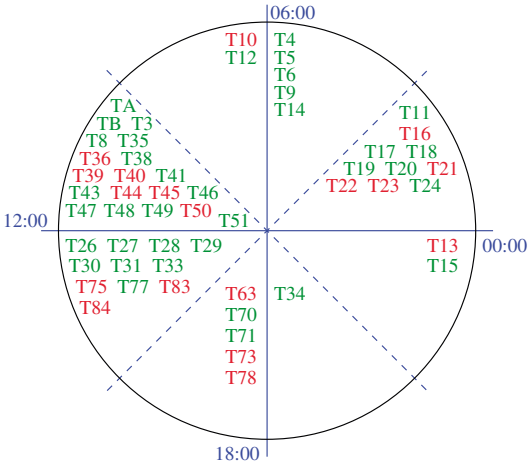


**Figure 7.** Deviations of Titan's induced magnetosphere from the draping picture: dependency on Saturnian local time. For local time sectors of 3 h duration, the figure displays the Titan flybys of categories "+" and "(+)" in green and the encounters of categories "0" and "-" in red. The 18 flybys assigned to the "oscillatory sheet" category (for which a different classification scheme was applied) are not considered in this figure.

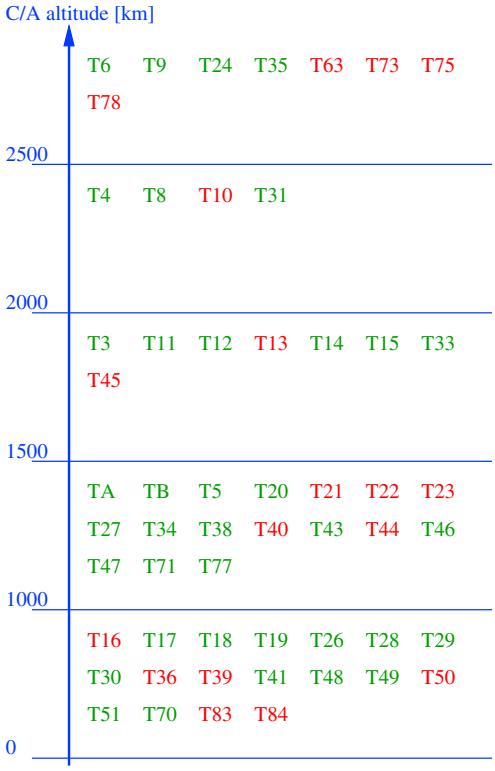


**Figure 8.** Deviations of Titan's induced magnetosphere from the draping picture: dependency on C/A altitude. The figure shows the relation between Titan flybys of different categories ("+"/"(+)" in green and "0"/"-" in red) and their C/A altitudes. The region between Titan's surface and 1 $R_T$ altitude ($\approx$2500 km) was binned in spherical shells of 500 km thickness. The 18 flybys of the "oscillatory sheet" category (for which a different classification scheme was applied) are not considered in this figure.

ambient flow was not aligned with the direction of ideal corotation, as also suggested by data from T9 *Bertucci et al.* [2007] and frequently required by numerical simulations to reproduce the magnetic field signatures seen near Titan [*Ma et al.*, 2006; *Simon et al.*, 2007b].

[79] In general, the draping pattern seen during Titan flybys which are assigned the labels "↓" and "weak" should be explainable in terms of a steady tilt of $\underline{u}_0$ against the corotation direction. Such a deviation of the incident flow direction from corotation is consistent with an initial analysis of CAPS data from the T15 flyby, suggesting that $\underline{u}_0$ can possess vertical and radial components which are only a factor of three to five smaller than the azimuthal component [*Sillanpää et al.*, 2011]. On the other hand, an enhanced disruption level of the draping pattern (labels "moderate" and "strong") suggests temporal variations in the incident flow conditions to play an important role in shaping Titan's induced magnetosphere during the flyby under consideration.

[80] The only flyby of the "*L–L*" type which cannot readily be explained in terms of the draping picture is T21. During this encounter, Cassini passed through the Titan interaction region from north to south and consequently, detected a region of negative $B_X$ perturbations, followed by an enhancement of $B_X$. However, subsequently, the MAG observed an additional dip in $B_X$, with its magnitude being comparable to the $B_X$ perturbation seen when the spacecraft entered the Titan interaction region. The origin of this signature is not evident, as it was detected at an altitude of about 1.7 $R_T$ where the plasma flow is not slowed down to stagnation, and, thus, magnetic field fossilization on time scales of a few hours is not possible [*Backes*, 2005; *Neubauer et al.*, 2006]. Possibly, this structure was generated by a localized jerk in the ambient flow speed.

[81] We have identified 18 Titan encounters during which quiet lobe-type fields were observed only on one side of C/A, while on the other side Cassini was embedded in the current sheet regime (categories "*L–Sh*" and "*Sh–L*," cf. third row in Table 4). It is remarkable to notice that during two thirds of these flybys, Titan's induced magnetosphere still featured no or only minor deviations from the stationary draping picture. This is even the case for encounters like T20 [*Simon et al.*, 2010a, Figure 6] during which Cassini was embedded in highly perturbed current sheet fields until about 1 h before C/A. The large number of flybys in the "+" and "(+)" categories implies that frequently, the varying background field conditions may cause only a minor "jitter" of Titan's induced magnetosphere, while leaving the large-scale draping structure nearly intact. This finding is also consistent with the hybrid simulation results by *Simon et al.* [2008a]. These authors demonstrated that when embedded in short-scale magnetospheric fluctuations (on the order of the ion gyroperiods), the large density of slow heavy ions near Titan is able to shield the tail against the ambient magnetospheric fluctuations. Instead of wobbling in synchronism with the background field fluctuations, the central plasma tail was found to align itself with the average background field direction, while only its outer flanks are continuously eroded by the time-varying background field.

[82] However, comparing the "*L–Sh*"/"*Sh–L*" encounters to the "*L–L*" case also shows that the relative number of Titan flybys with a severely disrupted induced magnetosphere has

also increased by a factor of three. It should be noted that while T10 possessed a C/A altitude of 2042 km, Cassini achieved C/A altitudes below 1800 km during the remaining five encounters assigned to the "0" category. When approaching Titan during these encounters, the spacecraft therefore passed through the regime where the plasma speed is sufficiently low and the magnetic Reynolds number is still large enough to permit field fossilization. Thus, the disruptions of the draping signals seen during these encounters may at least partially represent a record of Titan's interaction with the time-varying background field.

[83] Even when Cassini was exposed to perturbed current sheet fields on both sides of C/A (category "*Sh–Sh*," see fourth row in Table 4), the MAG detected only weak deviations from the steady-state draping picture during more than half of the Titan encounters. A possible reason is that within the current sheet, only the $B_x$ and $B_y$ components (in TIIS coordinates) exhibit short-scale fluctuations around $B_{x,y} = 0$, whereas the orientation of the north-south component ($B_z$) remains unaffected by the sheet motion and $|B_z|$ is also nearly constant. This behavior is well illustrated by magnetic field data acquired outside the Titan interaction region, e.g., during the T33 flyby (cf. Figure 10 in *Simon et al*. [2010a]). In this sense, the constant orientation of $B_z$—which during flybys within Saturn's current sheet is also the strongest component of the background field—may impose a stabilizing effect on the structure of Titan's induced magnetosphere.

[84] The constancy of $B_z$ during current sheet fluctuations may also be a possible reason why MAG data from numerous flybys of the "*L–Sh*" category (i.e., the onset of the ambient magnetospheric fluctuations coincided with Cassini's passage through the near-Titan region) still reveal a well-defined draping pattern. For this case, the findings of *Simon et al*. [2008a] furthermore imply that the ambient field fluctuations require a certain time to penetrate from the periphery to the inner regions of Titan's heavy ion plasma mantle and tail, i.e., the reaction of the induced magnetosphere to a sudden commencement of ambient field fluctuations occurs somewhat retarded.

[85] *Ulusen et al*. [2012] compared magnetic field observations from nine selected Titan flybys to the output of an MHD simulation for Voyager-type upstream conditions and came to similar conclusions. However, these authors also suggested that for noon local time conditions and flybys of the "*Sh–Sh*" type, the idealized draping picture is applicable only above altitudes of about 1800 km, whereas strong deviations from measurements are restricted to the region below that altitude. Our classification, on the other hand, indicates that there are numerous Titan flybys around noon, belonging to the *Sh–Sh* type and possessing a C/A altitude of *below* 1800 km, which nonetheless match the picture of ideal field line draping quite well: encounters T27, T28, T29, T30, T38, T47, T48, T49, T51, and T77 were all assigned to the "+" or the "(+)" category. Possible reasons for this discrepancy to the findings of *Ulusen et al*. [2012] may stem from our application of quantitatively rigid criteria to assess the level of deviation between the draping picture and observations. The study by *Ulusen et al*. [2012] does not provide a quantitative definition of "weak" and "strong" deviations between model output and MAG observations. Besides, as *Ulusen et al*. [2012] also point out, it is not clear to what degree a *single* MHD simulation run—based on Voyager-type input conditions—is able to suitably represent the incident flow conditions during the *series* of nine Titan flybys considered in their study.

[86] However, the *Sh–Sh* type is also the first one to encompass two Titan encounters during which an unambiguous identification of the moon's induced magnetosphere in MAG data was not possible at all (see fourth row, fifth column in Table 4). The trajectory of the T75 encounter featured a strong similarity to T9, an equatorial passage through Titan's midrange magnetotail which has been extensively discussed in the literature [*Bertucci et al*., 2007; *Coates et al*., 2007; *Kallio et al*., 2007; *Ma et al*., 2007; *Simon et al*., 2007b; *Szego et al*., 2007]. During both flybys, Cassini intersected Titan's geometric plasma wake in the ($z = 0$) plane (TIIS coordinates) at a C/A altitude of about 4 $R_T$, with the spacecraft moving mainly in ($-y$) direction. However, during T9 the MAG instrument observed a pronounced bipolar draping signature around C/A (peak magnitude $|\delta B_x| \approx 6$ nT, i.e., comparable to the background field strength), while no discernable sign of the Titan interaction was visible in MAG data from T75.

[87] We can only speculate that during T75, Titan's induced magnetotail was bent away from the flyby trajectory due to strong deviations of the incident flow direction from stationary corotation. In any case, both the T9 observations and results from various models (see above) suggest that under steady upstream conditions, Titan's magnetotail possesses an extension of more than 7 $R_T$ in ($+X$) direction. Hence, Cassini should have encountered a measurable magnetic field perturbation along the T75 trajectory. In a similar way, MAG data from the wakeside T73 flyby (C/A altitude $\approx 3$ $R_T$) did not reveal any clear signatures of the Titan interaction. While T9 occurred in the dawn sector of Saturn's magnetosphere (03:00 Saturnian local time), Titan was located in the dusk sector ($\approx$ 15:00 local time) during T73 as well as T75. Further passages through Titan's midrange magnetotail are required to clarify whether the discrepancies between MAG data from these encounters may be regarded an indication of a dawn–dusk asymmetry in the ambient flow direction near Titan's orbit.

[88] Finally, let us have a brief look at the flybys during which Titan was exposed to strong north-south sweeps of Saturn's magnetodisk current sheet (bottom row in Table 4). The ambient magnetic field conditions during the T54 encounter, as depicted in Figures 8 and 9 of *Simon et al*. [2010a], may be regarded a prototypical example of this flyby category. During almost half the flybys of this type, the magnitude of the distortions caused by Titan's local plasma interaction was comparable to or even exceeded by the ambient magnetospheric fluctuations. In such a perturbed magnetic environment, the signatures of Titan's local plasma interaction may be completely obscured, or an unambiguous discrimination between the Titan interaction and ambient magnetospheric fluctuations that occurred coincidentally is not feasible. Only during flybys T53, T55, T57, T59, T60, T61, T65, T68, and T69 the magnitude of the ambient magnetospheric fluctuations within a $\pm 8$ h interval around C/A was clearly exceeded by the Titan-related field distortion.

[89] Figure 7 displays the distribution of Titan flybys assigned to categories "0" and "-" (denoted in red) within the different local time sectors of Saturn's magnetosphere. Due to the proximity of Titan's orbit to Saturn's magnetopause in the dayside magnetosphere [*Achilleos et al*., 2008;

*Wei et al*., 2009], one would expect to encounter perturbed conditions within the moon's induced magnetosphere more frequently around noon local time. However, the available observations show no clear indication of such a behavior. In the dayside magnetosphere (06:00–18:00 local time), 13 out of 37 Titan flybys (i.e., 35%) were found to belong to the "0" or the "-" categories, while a similar fraction of 28 % was identified in the nightside magnetosphere (18:00–06:00 local time). As suggested by *Wei et al*. [2009], Titan itself may exert some level of control on the location of Saturn's dayside magnetopause with respect to its orbit. These authors demonstrated that near noon local time, Saturn's magnetopause can more frequently be found inside Titan's orbit with the moon absent than with it present. Thus, during Titan flybys around noon local time, the presence of the moon may keep Saturn's magnetopause at some distance to the moon's orbit, thereby also reducing the intensity of the perturbations seen within its induced magnetosphere.

[90] We have identified 18 Titan flybys during which the moon was exposed to strong north-south oscillations of Saturn's current sheet and the notion of a steady-state field line draping is therefore not applicable. It is interesting to notice that all these flybys occurred between 15:00 and 00:00 local time, with two thirds of them confined to a narrow region of the premidnight sector (21:00–00:00).

[91] Although below altitudes of about 2000 km, the field fossilization mechanism is potentially able to obscure signatures of Titan's interaction with the average background field, MAG data from only 14 out of the 44 Titan flybys with C/A below that altitude (i.e., less than one third) reveal substantial deviations from the draping picture (categories "0" and "-," see Figure 8). As pointed out by *Simon et al*. [2010a], all available information on the lifetime of fossil magnetic fields is so far based on the analysis of MAG data from the T32 magnetosheath excursion. However, the lifetime of fossil field signatures depends significantly on the location relative to Titan [*Simon et al*., 2010a; *Neubauer et al*., 2010]. C/A of T32 occurred in the Saturn-facing hemisphere of Titan and at high northern latitudes. Among the flybys with C/A altitudes between 1000 km and 2000 km that did *not* occur in Saturn's quiet magnetodisk lobes and show extitno strong signs of fossil fields, there is not a single one that sampled the same region as T32. For instance, encounters TA, TB, T3, T15, T20, and T77 had their C/A point located in Titan's wake, while T5, T33, T34, and T71 occurred upstream of the moon. The apparent absence of fossil magnetic field signatures along the trajectories of these encounters—despite the perturbed ambient magnetospheric field conditions—may indeed point towards a spatial inhomogeneity in the "efficiency" of the field storage mechanism. Especially for wakeside encounters, fossil field signatures may also have been partially smoothed out due to diffusion processes.

[92] In general, the datasets from the available Titan flybys do *not* point towards a clear increase of the disruptions inside Titan's induced magnetosphere with the disturbance level of the ambient field. On the one hand, T21 is the so far only encounter with quiet, lobe-type fields on both sides of C/A that was assigned to the "0"/"-" categories. On the other hand, however, there are also numerous Titan flybys with perturbed ambient field conditions during which no or only minor deviations from the draping picture were observed. Since the number of upcoming Titan flybys is rather limited, we do not expect this picture to change drastically until the end of Cassini's tour in the Saturnian system.

## 7. Summary and Concluding Remarks

[93] We have conducted a survey of Cassini magnetic field data acquired within Titan's induced magnetosphere during encounters TA–T85 (July 2004–July 2012). Our purpose was to identify those Titan flybys during which the observed perturbation signatures can be explained in terms of the idealized, stationary picture of field line draping around the moon's ionosphere. We also searched for a possible correlation between the disturbance level of the ambient magnetospheric field and the deviations from the steady-state draping picture.

[94] In our preceding studies, we applied a set of classification criteria to the radial magnetic field component ($B_y$ in TIIS coordinates), allowing a discrimination between Saturn's magnetodisk current sheet and lobe-type fields *outside* the Titan interaction region [*Simon et al*., 2010a, 2010b]. Expanding on this work, we have introduced two criteria that assess how strong the observed distortions of the flow-aligned ($B_x$) component *within* the interaction region deviate from the draping picture. After transforming the magnetic field data from TIIS ($x$,$y$,$z$) to the DRAP system ($X$,$Y$,$Z$) introduced by *Neubauer et al*. [2006], we first analyze whether the sign of the observed $B_X$ perturbations is in agreement with theoretical expectations. If the ambient magnetic field component $B_{0,X}$ along the corotation direction is negligible, the polarity reversal layer between Titan's magnetic lobes coincides with the ($Z = 0$) plane, whereas it is slightly tilted with respect to this plane in the case of $B_{0,X} \neq 0$. Second, we inspect the draping signature seen by Cassini for superimposed disruptions which may arise, e.g., from dynamics of Titan's magnetotail due to nonstationary incident flow conditions [*Simon et al*., 2008a], fossil magnetic fields [*Neubauer et al*., 2006; *Bertucci et al*., 2008], or neutral winds at low altitudes [*Cravens et al*., 2010]. We quantify the magnitude of these additional perturbations compared to the primary draping signal.

[95] Based on these two criteria, each Titan flyby is assigned to one of four categories: "+" means that the field perturbations detected within the moon's induced magnetosphere show no noticeable deviations from the steady-state draping picture. The $B_X$ perturbations seen during a flyby of the "(+)" category are still in qualitative agreement with the draping picture, but they also reveal non-negligible deviations, such as the polarity reversal layer being shifted into the "wrong" half space or fluctuations superimposed on the draping signal. During a flyby of the "0" category, the MAG still detected a perturbation around C/A that is associated with the Titan interaction. However, the magnetic field perturbations can no longer be explained in terms of the stationary draping picture, possibly due to significant contributions of fossil fields to the interaction signal. For a flyby assigned to the fourth category ("-"), an unambiguous identification of the Titan-related draping signature is either prevented by the high fluctuation level of the ambient magnetospheric field, or MAG data show no perturbations at all around C/A to Titan. For flybys that occurred during a current sheet sweep through Titan's orbital plane—i.e., a reversal in the signs of $B_x$ and $B_y$ occurred during the

Titan encounter—a less rigid classification criterion was introduced.

[96] By applying these criteria to MAG data from the available Titan encounters, we came to the following results:

[97] 1. So far, there are 55 Titan flybys which could potentially match the steady-state draping picture, since they occurred inside Saturn's magnetosphere and no intense current sheet sweeps were observed around C/A.

[98] 2. Only during one third of these encounters, the MAG detected severe deviations from the concept of steady-state draping (categories "0" and "-").

[99] 3. When Cassini was embedded in quiet, lobe-type fields on both sides of C/A, the field signatures seen within Titan's induced magnetosphere can well be explained in terms of steady-state draping of the average background field around the ionosphere.

[100] 4. Even when distorted current sheet fields were detected on one or even both sides of C/A, MAG data from more than 60 % of the available Titan flybys are still in qualitative agreement with the draping picture. During these flybys, "jitter" of the tail due to ambient magnetospheric perturbations or fossil field signatures has imposed only weak disruptions on the draping pattern. Titan's induced magnetosphere seems to be stabilized by the north-south component of the background field which is only weakly affected by the dynamics of Saturn's current sheet.

[101] 5. Only when C/A of an encounter coincides with a sweep of Saturn's oscillatory current sheet through the interaction region, the Titan signature is frequently obscured by the ambient magnetospheric fluctuations.

[102] 6. Magnetic field data from the available flybys do *not* indicate a dependency of the disruptions in Titan's induced magnetosphere on Saturnian local time. So far, the fraction of flybys in Saturn's dayside magnetosphere that can be explained in terms of field line draping is nearly the same as in the nightside magnetosphere.

[103] 7. Even at altitudes below 1800 km where the plasma speeds become sufficiently low to permit magnetic field fossilization, MAG data from numerous Titan flybys still match the steady-state draping picture reasonably well. Especially, this conclusion remains valid when Cassini detected perturbed current sheet fields on both sides of C/A.

[104] 8. So far, T70 is the only Titan encounter of the entire Cassini tour which matches the idealized ambient field conditions frequently applied in the pre-Cassini era (background magnetic field homogeneous, stationary and perpendicular to the moon's orbital plane). Besides, MAG data acquired during T70 within the interaction region can be explained in terms of field line draping, accompanied by a passage through Titan's magnetic ionopause region.

[105] In this study, we have applied the observed $B_x$ perturbations to identify deviations in the structure of Titan's induced magnetosphere from the steady-state draping picture. However, based on magnetic field measurements alone, it is not possible to identify the sources of these deviations for a specific flyby scenario. Especially, the impact of time-varying upstream conditions on the geometry of Titan's induced magnetosphere and their "storage" as fossil fields is still not well understood. Although initial real-time hybrid simulations succeeded in identifying several general characteristics of Titan's magnetotail in an oscillatory magnetic environment and during a change of the incident flow direction [*Simon et al*., 2008a; *Müller et al*., 2010], an application of such a time-dependent simulation approach to quantitatively analyze specific flyby scenarios is not yet feasible.

[106] On the one hand, a systematic catalogue of the ambient flow conditions—especially the *direction* of the incident magnetospheric plasma—during Cassini's Titan encounters is so far not available in the peer-reviewed literature. For the definition of the DRAP system in our study, we have assumed a purely azimuthal upstream velocity. This assertion might come into conflict with the fact that Saturn's current sheet is flapping up and down past Titan, thereby presumably affecting the nonazimuthal components of $\underline{u}_0$. Further studies of the incident flow velocity near Titan's orbit—expanding on the work of *Sillanpää et al*. [2011]—are therefore required for a sophisticated characterization of the upstream flow conditions.

[107] On the other hand, even if a more complete characterization of the incident flow parameters could be derived from measurements, their inclusion in a time-dependent, local plasma simulation will likely be confronted with the current numerical limitations of the model [*Müller et al*., 2010]. As recently discussed in the literature, a promising approach to this problem may be represented by two-body simulations, simultaneously treating the interaction between Saturn's magnetic field and the solar wind as well as Titan's interaction with the resulting magnetospheric configuration [*Winglee et al*., 2009; *Snowden et al*., 2011a, 2011b]. However, these combined simulations so far lack a sufficient grid resolution near Titan to reproduce, e.g., magnetic fine structures within the moon's ionosphere.

[108] Finally, we would briefly like to dwell on the issues associated with an application of the *dynamic* DRAP system of *Neubauer et al*. [2006] to the Titan flybys. First and foremost, the dynamic DRAP system introduced by these authors assumes the background field to possess constant (albeit different) values $\underline{B}_{0,i}$ and $\underline{B}_{0,o}$ in the inbound (subscript i) and outbound (subscript o) regions of the Titan flybys and also assumes a *linear* variation from $\underline{B}_{0,i}$ to $\underline{B}_{0,o}$ during the passage through the interaction region. The assumption of a linear variation from one constant value to another can certainly only be applied when the magnetic field on both sides of the interaction region is rather quiet, i.e., if it does not show strong signs of superimposed magnetospheric perturbations. This requirement was reasonably well fulfilled during the three encounters (TA, TB, T3) analyzed by *Neubauer et al*. [2006].

[109] In general, one would expect the assumption of a linear variation to be justified for flybys with lobe-type fields on both sides of C/A (category *L–L*). However, for the bulk of the flybys assigned to this category (90 %), we were able to demonstrate that the application of a *dynamic* DRAP system is not even necessary, but the pre-Cassini picture (i.e., applying a *static* DRAP system defined by constant $\underline{B}_0$) already does an excellent job in organizing the MAG data. We would also like to emphasize that our classification results for TA, TB, and T3 (derived in static DRAP coordinates) are in full agreement with the findings of *Neubauer et al*. [2006] who analyzed these data in a dynamic DRAP system.

[110] For the overwhelming number of Titan flybys, perturbed current sheet fields were observed near C/A. In such

scenarios, the concept of $\underline{B}_0$ varying linearly between two "anchor values" $\underline{B}_{0,i}$ and $\underline{B}_{0,o}$ is not applicable, since the variation of $\underline{B}_0$ during Cassini's passage through the interaction region is not known and cannot be reconstructed from the data. Magnetic field observations of current sheet dynamics near Titan's orbit during numerous flybys (e.g., T21 and T54, see *Simon et al*. [2010a]) suggest that the assumption of a linear variation is not applicable at all in these cases, thereby rendering the method introduced by *Neubauer et al*. [2006] infeasible.

[111] **Acknowledgments.** Masaki Fujimoto thanks the reviewers for their assistance in evaluating this paper. The work of S $^2$ and J.S. was financially supported by the Deutsche Forschungsgemeinschaft (DFG) under grant SI1753/1-1. S $^2$ would like to thank Hendrik Kriegel (TU Braunschweig) for careful inspection of the manuscript and for valuable comments.

## References

Achilleos, N., C. S. Arridge, C. Bertucci, C. M. Jackman, M. K. Dougherty, K. K. Khurana, and C. T. Russell (2008), Large-scale dynamics of Saturn's magnetopause: Observations by Cassini, *J. Geophys. Res.*, *113*, A11–209, doi:10.1029/2008JA013265.

Arridge, C. S., C. T. Russell, K. K. Khurana, N. Achilleos, S. W. H. Cowley, M. K. Dougherty, D. J. Southwood, and E. J. Bunce (2008a), Saturn's magnetodisc current sheet, *J. Geophys. Res.*, *113*, A04–214, doi:10.1029/2007JA012540.

Arridge, C. S., K. K. Khurana, C. T. Russell, D. J. Southwood, N. Achilleos, M. K. Dougherty, A. J. Coates, and H. K. Leinweber (2008b), Warping of Saturn's magnetospheric and magnetotail current sheets, *J. Geophys. Res.*, *113*, A08–217, doi:10.1029/2007JA012963.

Arridge, C. S., et al. (2011a), Periodic motion of Saturn's nightside plasma sheet, *J. Geophys. Res.*, *116*, A11–205, doi:10.1029/2011JA016827.

Arridge, C. S., et al. (2011b), Upstream of Saturn and Titan, *Space Science Rev.*, *162*(1–4), 25–83, doi:10.1007/s11214-011-9849-x.

Arridge, C. S., N. Achilleos, and P. Guio (2011c), Electric field variability and classifications of Titan's magnetoplasma environment, *Ann. Geophys.*, *29*(7), 1253–1258, doi:10.5194/angeo-29-1253-2011.

Backes, H. (2005), Titan's interaction with the Saturnian magnetospheric plasma, Ph.D. thesis, Universität zu Köln.

Backes, H., et al (2005), Titan's magnetic field signature during the first Cassini encounter, *Science*, *308*(5724), 992–995, doi:10.1126/science.1109763.

Bertucci, C., F. M. Neubauer, K. Szego, J.-E. Wahlund, A. J. Coates, M. K. Dougherty, D. T. Young, and W. S. Kurth (2007), Structure of Titan's mid-range magnetic tail: Cassini magnetometer observations during the T9 flyby, *Geophys. Res. Lett.*, *34*(24), L24S02, doi:10.1029/2007GL030865.

Bertucci, C., et la. (2008), The magnetic memory of Titan's ionized atmosphere, *Science*, *321*(5895), 1475–1478, doi: 10.1126/science.1159,780.

Bertucci, C., B. Sinclair, N. Achilleos, P. Hunt, M. K. Dougherty, and C. S. Arridge (2009), The variability of Titan's magnetic environment, *Planet. Space Sci.*, *57*(14–15), 1813–1820, doi:10.1016/j.pss.2009.02.009.

Coates, A. J., F. J. Crary, D. T. Young, K. Szego, C. S. Arridge, Z. Bebesi, E. C. Sittler, R. E. Hartle, and T. W. Hill (2007), Ionospheric electrons in Titan's tail: Plasma structure during the Cassini T9 encounter, *Geophys. Res. Lett.*, *34*(24), L24S05, doi:10.1029/2007GL030919.

Cravens, T. E., et al. (2010), Dynamical and magnetic field time constants for Titan's ionosphere: Empirical estimates and comparisons with Venus, *J. Geophys. Res.*, *115*, A08–319, doi:10.1029/2009JA015050.

Dougherty, M. K., et al. (2004), The Cassini magnetic field investigation, *Space Science Reviews*, *114*, 331–383, doi:10.1007/s11214-004-1432-2.

Kallio, E., I. Sillanpää, and P. Janhunen (2004), Titan in subsonic and supersonic flow, *Geophys. Res. Lett.*, *31*(15), L15–703, doi:10.1029/2004GL020344.

Kallio, E., I. Sillanpää, R. Jarvinen, P. Janhunen, M. Dougherty, C. Bertucci, and F. Neubauer (2007), Morphology of the magnetic field near Titan: Hybrid model study of the Cassini T9 flyby, *Geophys. Res. Lett.*, *34*(24), L24S09, doi:10.1029/2007GL030827.

Ledvina, S. A., J. G. Luhmann, S. H. Brecht, and T. E. Cravens (2004), Titan's induced magnetosphere, *Adv. Space Res.*, *33*(11), 2092–2102, doi:10.1016/j.asr.2003.07.056.

Luhmann, J. G. (1996), Titan's ion exosphere wake: A natural ion mass spectrometer?, *J. Geophys. Res.*, *101*(E12), 29,387–29,393, doi:10.1029/96JE03307.

Ma, Y.-J., A. F. Nagy, T. E. Cravens, I. V. Sokolov, K. C. Hansen, J.-E. Wahlund, F. J. Crary, A. J. Coates, and M. K. Dougherty (2006), Comparisons between MHD model calculations and observations of Cassini flybys of Titan, *J. Geophys. Res.*, *111*, A05–207, doi:10.1029/2005JA011481.

Ma, Y.-J., et al. (2007), 3D global multi-species Hall-MHD simulation of the Cassini T9 flyby, *Geophys. Res. Lett.*, *34*, L24S10, doi:10.1029/2007GL031627.

Ma, Y.-J., et al. (2009), Time-dependent global MHD simulations of Cassini T32 flyby: From magnetosphere to magnetosheath, *J. Geophys. Res.*, *114*, A03–204, doi:10.1029/2008JA013676.

Ma, Y. J., et al.(2011), The importance of thermal electron heating in Titan's ionosphere: Comparison with Cassini T34 flyby, *J. Geophys. Res.*, *116*, A10–213, doi:10.1029/2011JA016657.

Müller, J., S. Simon, U. Motschmann, K. H. Glassmeier, J. Saur, J. Schuele, and G. J. Pringle (2010), Magnetic field fossilization and tail reconfiguration in Titan's plasma environment during a magnetopause passage: 3D adaptive hybrid code simulations, *Planet. Space Sci.*, *58*(12), 1526–1546, doi:10.1016/j.pss.2010.07.018.

Németh, Z., K. Szego, Z. Bebesi, G. Erdős, L. Foldy, A. Rymer, E. C. Sittler, A. J. Coates, and A. Wellbrock (2011), Ion distributions of different Kronian plasma regions, *J. Geophys. Res.*, *116*, A09–212, doi:10.1029/2011JA016585.

Neubauer, F. M., D. A. Gurnett, J. D. Scudder, and R. E. Hartle (1984), Titan's magnetospheric interaction, in *Saturn*, edited by T. Gehrels and M. S. Matthews, pp. 760–787, University of Arizona Press, Tucson, Arizona.

Neubauer, F. M., et al. (2006), Titan's near magnetotail from magnetic field and plasma observations and modelling: Cassini flybys TA, TB and T3, *J. Geophys. Res.*, *111*, A10–220, doi:10.1029/2006JA011676.

Neubauer, F. M., A. Hoerdt, A. Wennmacher, S. Simon, C. Bertucci, and M. K. Dougherty (2010), Fossil magnetic fields due to Titan's plasma interaction revisited: The role of the electric conductivities in the ionosphere and in Titan's interior, American Geophysical Union, Fall Meeting 2010, abstract #SM13D-07.

Rymer, A. M., H. T. Smith, A. Wellbrock, A. J. Coates, and D. T. Young (2009), Discrete classification and electron energy spectra of Titan's varied magnetospheric environment, *Geophys. Res. Lett.*, *36*, L15–109, doi: 10.1029/2009GL039427.

Sillanpää, I., D. T. Young, F. Crary, M. Thomsen, D. Reisenfeld, J.-E. Wahlund, C. Bertucci, E. Kallio, R. Jarvinen, and P. Janhunen (2011), Cassini Plasma Spectrometer and hybrid model study on Titan's interaction: Effect of oxygen ions, *J. Geophys. Res.*, *116*, A07–223, doi:10.1029/2011JA016443.

Simon, S., and U. Motschmann (2009), Titan's induced magnetosphere under non-ideal upstream conditions: 3D multi-species hybrid simulations, *Planet. Space Sci.*, *57*(14–15), 2001–2015, doi:10.1016/j.pss.2009.08.010.

Simon, S., A. Boesswetter, T. Bagdonat, U. Motschmann, and K.-H. Glassmeier (2006), Plasma environment of Titan: A 3-d hybrid simulation study, *Ann. Geophys.*, *24*(3), 1113–1135.

Simon, S., A. Boesswetter, T. Bagdonat, U. Motschmann, and J. Schuele (2007a), Three-dimensional multispecies hybrid simulation of Titan's highly variable plasma environment, *Ann. Geophys.*, *25*(1), 117–144.

Simon, S., G. Kleindienst, A. Boesswetter, T. Bagdonat, U. Motschmann, K.-H. Glassmeier, J. Schuele, C. Bertucci, and M. K. Dougherty (2007b), Hybrid simulation of Titan's magnetic field signature during the Cassini T9 flyby, *Geophys. Res. Lett*., *34*(L24S08), doi:10.1029/2007GL029967.

Simon, S., U. Motschmann, and K.-H. Glassmeier (2008a), Influence of non-stationary electromagnetic field conditions on ion pick-up at Titan: 3-d multispecies hybrid simulations, *Ann. Geophys.*, *26*(3), 599–617.

Simon, S., U. Motschmann, G. Kleindienst, J. Saur, C. Bertucci, M. Dougherty, C. Arridge, and A. Coates (2009a), Titan's plasma environment during a magnetosheath excursion: Real-time scenarios for Cassini's T32 flyby from a hybrid simulation, *Ann. Geophys.*, *27*(2), 669–685.

Simon, S., J. Saur, F. Neubauer, U. Motschmann, and M. Dougherty (2009b), Plasma wake of Tethys: Hybrid simulations versus Cassini MAG data, *Geophys. Res. Lett.*, *36*(4), L04–108, doi:10.1029/2008GL036943.

Simon, S., A. Wennmacher, F. Neubauer, C. Bertucci, H. Kriegel, J. Saur, C. Russell, and M. Dougherty (2010a), Titan's highly dynamic magnetic environment: A systematic survey of Cassini magnetometer observations from flybys TA–T62, *Planet. Space Sci.*, *58*(10), 1230–1251, doi:10.1016/j.pss.2010.04.021.

Simon, S., A. Wennmacher, F. Neubauer, C. Bertucci, H. Kriegel, J. Saur, C. Russell, and M. Dougherty (2010b), Dynamics of Saturn's magnetodisk near Titan's orbit: Comparison of Cassini magnetometer observations from real and virtual Titan flybys, *Planet. Space Sci.*, *58*(12), 1625–1635, doi:10.1016/j.pss.2010.08.006.

Simon, S., U. Motschmann, G. Kleindienst, K.-H. Glassmeier, C. Bertucci, and M. K. Dougherty (2008b), Titan's magnetic field signature during the Cassini T34 flyby: Comparison between hybrid simulations and MAG data, *Geophys. Res. Lett.*, *35*, L04107, doi:10.1029/2007GL033056.

Snowden, D., R. Winglee, and A. Kidder (2011a), Titan at the edge Part I: Titan's interaction with Saturn's magnetosphere in the pre-noon sector, *J. Geophys. Res.*, *116*, A08–229, doi:10.1029/2011JA016435.

Snowden, D., R. Winglee, and A. Kidder (2011b), Titan at the edge Part II: A global simulation of Titan exiting and re-entering Saturn's magnetosphere at 13.6 SLT, *J. Geophys. Res.*, *116*, A08–230, doi:10.1029/2011JA016436.

Szego, K., Z. Bebesi, C. Bertucci, A. J. Coates, F. Crary, G. Erdos, R. Hartle, E. C. Sittler, and D. T. Young (2007), Charged particle environment of Titan during the T9 flyby, *Geophys. Res. Lett.*, *34*(24), L24S03, doi:10.1029/2007GL030677.

Ulusen, D., J. G. Luhmann, Y. J. Ma, K. E. Mandt, J. H. Waite, M. K. Dougherty, J. E. Wahlund, C. T. Russell, T. E. Cravens, N. J. T. Edberg, and K. Agren (2012), Comparisons of Cassini flybys of the Titan magnetospheric interaction with an MHD model: Evidence for organized behavior at high altitudes, *Icarus*, *217*(1), 43–54, doi:10.1016/j.icarus.2011.10.009.

Wei, H. Y., C. T. Russell, A. Wellbrock, M. K. Dougherty, and A. J. Coates (2009), Plasma environment at Titan's orbit with Titan present and absent, *Geophys. Res. Lett.*, *36*(23), L23–202, doi:10.1029/2009GL041048.

Wei, H. Y., C. T. Russell, M. K. Dougherty, F. M. Neubauer, and Y. J. Ma (2010), Upper limits on Titan's magnetic moment and implications for its interior, *J. Geophys. Res.*, *115*, E10–007, doi: 10.1029/2009JE003,538.

Winglee, R., D. Snowden, and A. Kidder (2009), Modification of Titan's ion tail and the Kronian magnetosphere: Coupled magnetospheric simulations, *J. Geophys. Res.*, *114*, A05–215, doi:10.1029/2008JA013343.